Spring 2012

Nano- and Micro-Second Electrical Pulsing of B16-F10 Mouse Melanoma Cells: Plasma Membrane and Sub-Cellular Organelle Changes

Yiling Chen
Old Dominion University

NANO- AND MICRO-SECOND ELECTRICAL PULSING OF B16-F10 MOUSE MELANOMA CELLS: PLASMA MEMBRANE AND SUB-CELLULAR ORGANELLE CHANGES

by

Yiling Chen
Bachelor of Medicine July 2001, Tianjin Medical University, China
M.S. August 2004, The University of Nottingham, United Kingdom

A Dissertation Submitted to the Faculty of
Old Dominion University in Partial Fulfillment of the
Requirements for the Degree of

DOCTOR OF PHILOSOPHY

BIOMEDICAL SCIENCES

OLD DOMINION UNIVERSITY
May 2012

Approved by:

R. James Swanson (Director)

Karl H. Schoenbach (Member)

Christopher J. Osgood (Member)

David Gauthier (Member)

ABSTRACT

NANO- AND MICRO-SECOND ELECTRICAL PULSING OF B16-F10 MOUSE MELANOMA CELLS: PLASMA MEMBRANE AND SUB-CELLULAR ORGANELLE CHANGES

Yiling Chen
Old Dominion University, 2012
Director: Dr. R. James Swanson

High electric field-treated cells are permeable to molecular dye through either opening of pores in the plasma membrane or other unknown processes which can disturb the membrane in an organized way. However, direct morphological evidence is lacking and responses of intracellular organelles are not clear. We used traditional chemical fixatives and biochemical techniques to capture cell membrane and organelle changes immediately after pulsing with high voltage electric field application. Different pulse durations, nanosecond (ns) and microsecond (μs), and field magnitudes, 60 kV/cm and 1.2 kV/cm, were applied to mouse melanoma B16-F10 cells. Two different ns durations (60 and 300 ns) with an electric field of 60 kV/cm and microsecond duration (100 μs) at 1.2 kV/cm were used in this study.

Morphological changes on plasma membranes and cell organelles were analyzed with transmission electron microscopy (TEM) immediately after one to six applied pluses. TEM micrographs demonstrated morphological changes in plasma membrane and mitochondrial structure for treated cells under certain pulse conditions. Additionally, B16-F10 cells were: 1) assessed post-pulse for membrane permeability and live/dead ratio using trypan blue; 2) monitored for mitochondrial membrane potential ($\Delta\psi m$) changes with JC-1, a voltage-sensitive mitochondrial dye; and 3) cultured for 24 hrs post-

pulse to determine long-term viability. Detailed cellular responses were evaluated based on the different electric fields, pulse duration, and number of pulses.

Cell membranes appeared to be unperturbed while mitochondrial membranes were negatively affected after the defined ns pulse treatments. Increasing the number of ns pulses introduced more mitochondrial abnormalities and led to decreased cellular viability. With fewer pulse numbers (1-2 pulses), mitochondrial morphology and $\Delta\psi m$ were similar to controls. With μs pulse duration, intracellular organelles were less disturbed than the cell membranes. Under high electric field (60 kV/cm), changes in cell membrane permeability and irregularity increased, while cell viability and mitochondrial potential decrease, both with the longer duration (300 ns vs. 60 ns) and with higher pulse numbers under the same duration. The low electric field (1.2 kV/cm) caused fewer changes to the cell membrane and intracellular organelles even though the pulse durations (100 μs vs. 300 or 60 ns) were longer.

Dedicated to my mother and father
who has always supported me.

ACKNOWLEDGMENTS

To reach the completion of my dissertation and subsequent PhD has been a long journey. Much has changed in the time I have been involved with this project. I owe my gratitude to many people who have contributed to the production and completion of this degree. To this select group, I would like to give special thanks, beginning with Dr. R. James Swanson. I could not have succeeded without his invaluable support. I really appreciate having him direct my course of study, candidate exam, research and defense. Dr. Swanson and his wife are more than teachers to me. I view them as my American parents.

I wish to thank my committee member Dr. David Gauthier for coaching me to the completion of the transmission electron microscopy experiments in his laboratory. He stimulated my further thinking of experimental design. I am extremely grateful for the assistance, generosity and advice I received from my friend, Dr. Wentia Ford who knew the answer to every question I have ever asked regarding my experiments. I am very grateful to the remaining members of my dissertation committee Dr. Christopher J. Osgood and Dr. Karl Schoenbach. Their academic support and input and personal cheering are greatly appreciated.

This research was supported by Dr. Swanson and his lab. I extend many thanks to Dr. Juergen Kolb, Dr. Shu Xiao and Dr. Beebe, who gave me a lot of help in my project. I would like to acknowledge them for numerous discussions and lectures during their courses that helped me improve my knowledge.

My graduate studies would not have been the same without the social and academic challenges and diversions provided by all my student-colleagues in ODU. Next

I would like to thank Dr. Xinhua Chen, or as I call her, my dear sister. I cannot begin to express my gratitude and feelings for this gregarious woman. We have laughed, cried and among other things, cursed together. Having met in this very doctoral program, Xinhua had first-hand knowledge of the dissertation process and what I was experiencing. In her I have a life-long friend and colleague. For all these reasons and many, many more, I am eternally grateful. Thank you Xinhua for being persistent and encouraging, for believing in me, and for the many precious memories along the way. I am particularly thankful to my friends Wei Ren, Fang Li, Liang Yu, Jie Zhuang, Jie Liu, Hongxia Jia, Carmony Hartwig and Eoin Whelan.

Of course no acknowledgments would be complete without giving thanks to my parents. Both have instilled many admirable qualities in me and given me a good foundation with which to meet life. They have taught me about hard work and self-respect, about persistence and about how to be independent. Both have always expressed how proud they are of me and how much they love me. I too am proud of them and love them very much.

Last, but certainly not least, I must acknowledge with deep thanks my husband, Xuyao Ni and my lovely son, Nathan Ni. Xuyao constantly asked me "are you done yet?" and affectionately referring to me as a 'professional student'. Thank you for your encouragement, support and most of all your humor. You kept things light and me smiling.

TABLE OF CONTENTS

Page

LIST OF FIGURES

CHAPTER 1

INTRODUCTION

1.1 Cell Membrane Structure and Function

1.1.1 Cell Outer Membrane

The cell membrane is a physical barrier that separates the inside of the cell from the extracellular environment (Alberts et al., 2002). This barrier is composed of a phospholipid bilayer embedded with membrane proteins and is associated with various cell functions (Figure 1). This membrane plays an essential role in cell adhesion, conductivity and signaling, and provides a surface for extracellular glycocalyx and intracellular cytoskeleton attachments (Alberts et al., 2002). The cell membrane is selectively permeable to ions and many organic molecules, therefore regulating what enters and exits the cell (Alberts et al., 2002). In addition, it facilitates the transportation of materials needed for cell survival.

Substance transportation across the membrane can be either passive or active. Passive movement requires no cellular energy but active movement requires energy to achieve directional transport. Apart from its structural properties, the cell membrane is also involved in many important cellular processes such as maintaining an ionic balance between the inside and outside of the membrane. The differential ionic potential can trigger the release of transmission signals within or between cells such as neurons and is

---

The dissertation journal model is *Cell*.

the driving force for the correct function of various membrane-embedded proteins. (Alberts et al., 2002).

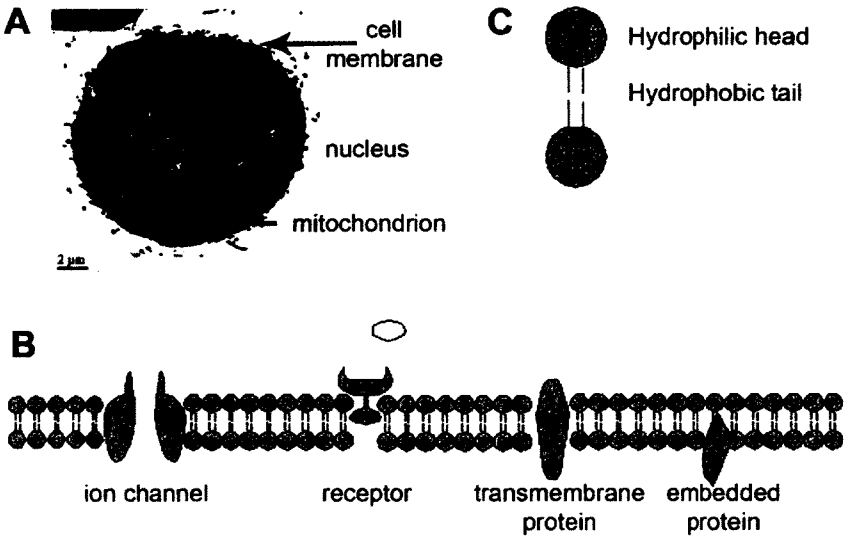

Figure 1. Image of a eukaryotic cell and structure of the lipid bilayer
(A) Image of a eukaryotic cell. Components such as cell membrane, nucleus, and mitochondrion are indicated by arrows.
(B) Schematic diagram of the cell membrane. The continuous lipid bilayer contains embedded proteins (such as ion channel and receptor) and glycolipid (not shown).
(C) Enlarged phospholipid molecules. The polar head group of phospholipids is facing the inside and outside environment while the hydrophilic tails are buried inside (Gardner and Boles, 2005).

The fundamental structural component of the cell membrane is the thin bilayer of amphipathic phospholipids, arranged in a highly organized configuration. The hydrophobic tail regions of phospholipids face inward and are in close contact with each other. They are protected from the external polar environment while the hydrophilic head groups face both the cytosol and the extracellular fluid. The entire lipid bilayer, which is continuous and spherical, forms through a self-assembly process with hydrophobic

interactions as the major driving force. Other forces such as van der Waals, electrostatic interactions, hydrogen bonds, and various non-specific, non-covalent interactions also contribute to the formation of the lipid bilayer (Singer and Nicolson, 1972). The unique composition of the cell membrane contributes to its description as a fluid mosaic model (Singer and Nicolson, 1972) in which the biological membrane is a two-dimensional liquid surface with lipid and protein molecules moving laterally along the surface (Alberts et al., 2002). On the other hand, the plasma membrane also contains stable structures or domains such as protein-protein complexes, lipid rafts, and "pickets and fences" formed by the actin-based cytoskeleton.

The special arrangement of hydrophobic tails sandwiched by hydrophilic heads makes it difficult for polar molecules to move across the cell membrane. Where hydrophobic molecules are capable of passive diffusion to cross this barrier with less difficulty, movement of polar molecules such as amino acids, nucleic acids, carbohydrates, proteins, and ions into and out of the cell are facilitated using transmembrane protein complexes, such as pores and gates.

1.1.2 Intracellular Membranes

Similar to the cell membrane, many intracellular organelles (e.g. nucleus, mitochondria, Golgi apparatus, etc.) which carry out various cellular functions inside the cell, are encapsulated by a membrane consisting of single or double lipid bilayer(s). Among them, the nuclear envelope (NE) (also known as the perinuclear envelope and nuclear membrane) contains double lipid bilayers, which act as a physical barrier separating the contents of the nucleus (DNA in particular) from the cytosol in eukaryotic

cells and have also been suggested to be involved in the organization and transcriptional activity of chromatin (Singer and Nicolson, 1972). Pores on the nuclear envelope regulate and facilitate the exchange of materials, such as transcription factors and RNA, between the nucleus and the cytoplasm. The outer NE membrane is a continuous structure with the rough endoplasmic reticulum (ER) and the inner NE membrane contains several inner nuclear membrane proteins. These two membranes are fused at the site of nuclear pore complexes (McBride et al., 2006).

The mitochondrion is a membrane-enclosed organelle that ranges from 0.5 to 10 micrometers (μm) in diameter and provides chemical energy for the cell. The adenosine triphosphate (ATP) generated by mitochondria not only acts as the energy source of the cell, but also as a coenzyme and is involved in many cellular processes (Henze and Martin, 2003). In addition, mitochondria are functional in cell signaling, cell differentiation, cell death, cell cycle control and cell growth (McBride et al., 2006). Certain human diseases such as cardiac dysfunction and aging have been suggested to be related to mitochondrial disorders (Gardner and Boles, 2005; Lesnefsky et al., 2001).

The mitochondrion also contains a double lipid bilayer structure, and each bilayer has its own properties and functions (Henze and Martin, 2003). These two membranes differ from the NE membrane based on their unique embedded membrane proteins and five compartments that are separated by the inner and outer membrane and carry out specialized functions (Figure 2). The first two components are the outer and inner membranes themselves. The space within the inner membrane is called the matrix while the space between the outer and inner membranes is the intermembrane space.

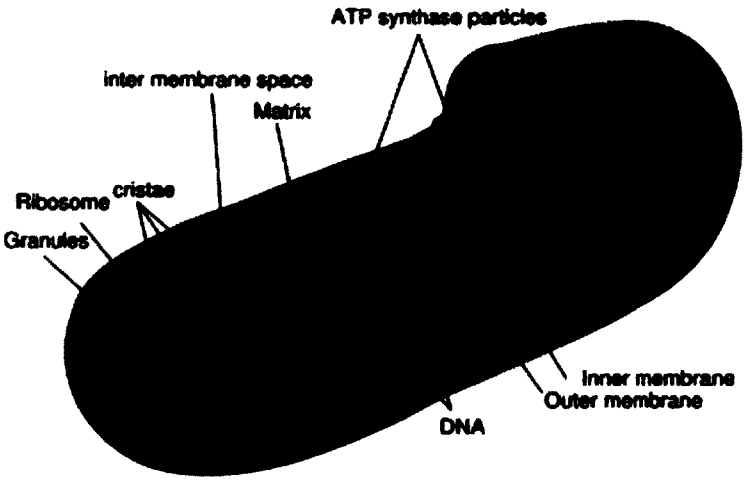

Figure 2. Anatomy of mitochondria (Mariana, 2006)
Mitochondrial membrane associated with structural components (outer and inner membrane, matrix, intermembrane space, and cristae) are listed.

The mitochondrion outer membrane acts as a physical barrier of the entire organelle. The protein to phospholipid ratio (by weight) is about 1:1 for the outer membrane which is similar to the eukaryotic plasma membrane. The membrane is permeable to molecules of 5000 Daltons or less with the aid of embedded channel-forming proteins called porins (Henze and Martin, 2003). Larger proteins can enter the mitochondrion through the translocase, an outer membrane embedded multi-subunit protein. By the recognition of a signaling sequence at the N-terminus, large proteins can be actively moved across the membrane (Herrmann and Neupert, 2000). The integrity of the mitochondrial outer membrane is essential and surface damages can lead to protein leakage from the intermembrane space into the cytosol, resulting in cell apoptosis (Chipuk et al., 2006). The mitochondrial outer membrane has also been found to be important in the calcium signaling and lipid transfer between the ER and mitochondria

(Hayashi et al., 2009). This functional role is achieved by forming structures called the mitochondria-associated ER-membrane (MAM), which physically connects the two structures.

The mitochondrion inner membrane is compartmentalized into numerous cristae which significantly expands its surface area and therefore enhances the efficiency of ATP production. Different types of cells have various ratios of the surface area and as a general trend, more cristae can be found for mitochondria in the cells that require large amounts of ATP, such as muscle cells.

1.2 Membrane Potential

Ionic concentration is different on the intracellular and extracellular sides of the cell plasma membrane due to the effect of membrane embedded ion channels and ion pumps that can regulate ion transport. This results in an electrical potential difference between the inside and outside of the membrane. This electrical potential differences across the membrane ($V_{interior} - V_{exterior}$) is known as the membrane potential. The membrane potential also allows cells such as neurons to transmit signals. Local potential change caused by the opening or closing of ion channels at one part of the membrane can be rapidly spread to other parts of the membrane.

All cells have a resting potential which is an electrical charge across the plasma membrane, with the interior of the cell negative with respect to the exterior. The size of the resting potential varies in different types of cells. Certain cells (e.g. muscle, heart, and nerve cells) can respond to internal or external stimulation to create an electric current and therefore are called excitable cells. On the contrary, for non-excitable cells

(e.g. fibroblasts, adipocites, and endothelial cells) and excitable cells in their resting states (i.e. without stimulation), the transmembrane potential remains at a relative stable value and is therefore noted as the resting potential.

Membrane potential is a characteristic property of the cell because of the sustained ionic concentration difference inside and outside the cell. For excitable cells, changes in membrane potential (i.e. ionic concentration changes) are controlled by a specific active transportation mechanism such as the Na^+/K^+-ATPase pump. External factors (chemical or electrical) which have an effect of membrane perturbation can also change the membrane potential by opening pores on the membrane and thus altering the ionic concentrations inside and outside the cell. Similarly, the intracellular organelle, mitochondria, also requires a membrane potential for its proper function. Significant changes in mitochondrial membrane potential are often associated with lethal effects, such as apoptosis (Beebe et al., 2002).

1.3 Electric Field Effects on Membrane (Electroporation)

Many factors can affect the structure and function of cellular membranes. These include chemical damage, radiation, and electric fields. Among them, the effect of electric fields exerted on cell membranes has been studied for many years and research investigating the electrical properties of cells began earlier than the development of the membrane hypothesis of cells (Crowley, 1973; Moore, 1969). Impacts of electric fields can be quantitatively understood by considering the cell as an electrical circuit (Joshi et al., 2001; Joshi et al., 2002; Joshi and Schoenbach, 2000). On one hand, the immediate electric field-cell interaction can be readily predicted once the values of all circuit

components are known. On the other hand, changes in cellular structures induced by electric fields can be determined by alterations in circuit components.

The cell has both capacitance and resistance properties. By adjusting ion concentration inside and outside the membrane with specific ion channels, the cell can store and release charge in an electric field. The lipid bilayer of the cell membrane has low conductivity while the cytoplasm within is moderately conductive. Therefore, the cell is a conductor enclosed by an insulating plasma membrane. Similar properties are demonstrated by intracellular organelles that are enclosed in a membrane.

The charging time of cell membrane is the time required for a cell to reach maximum electrical potential and this varies according to the different electrical parameters of the cell and the medium in which it is suspended. For spherical cells with an ideal dielectric distribution on the surface membrane, the charging time (τ_c) can be calculated as:

$$\tau_c = (\rho_c + 0.5\rho_a) \cdot C_m \cdot D \text{ (Cole, 1937)} \qquad (1)$$

Here ρ_c is the resistivity of the cytoplasm, ρ_a is the resistivity of the suspension medium, C_m is capacitance of the surface membrane per unit area, and D is the cell diameter. For a cell size of 10 μm in diameter, cytoplasm and medium resistivity of 100 Ωcm, and a membrane capacitance of 1 μF/cm^2, the membrane charging time is 150 ns.

Direct current electric field pulses with durations longer than the charging time of the plasma membrane will charge the outer membrane. While charging of subcellular organelles can occur at the same time, the accumulated potential differences across their membranes and the resulting effects can only become significant with a much reduced pulse rise time. For human cells, the charging times for the plasma membrane are

generally within sub-microseconds range. Earlier studies of pulsed electric field applications are mostly focused on charging the outer membrane of biological cells with pulses greater than microseconds (Weaver, 2000). Therefore, with microsecond or greater pulse durations, the potential differences across inner membranes can be neglected.

Another consideration for determining the effect of an electric field on cells is the applied field strength. The application of a high electric field to cells or tissues permeabilizes the cell membrane and is thought to produce aqueous pores in the lipid bilayer (Crowley, 1973; Dimitrov, 1984; Glaser et al., 1988; Needham and Hochmuth, 1989; Teissi et al., 1999; Zimmermann, 1996; Zimmermann et al., 1976). This process, first observed for planar bilayer lipid membranes (Abiror *et al.*, 1979; Benz *et al.*, 1979), is referred to as membrane breakdown, electropermeabilization, or electroporation (Tsong, 1991; Weaver, 1995). Although the mechanism of electroporation is not fully understood, this technique has been widely used for 25 years for many applications, such as intracellular delivery of drugs, dyes, and plasmids, and in cancer therapy and immune stimulation (Heller and Heller, 2006; Sersa et al., 2008; Tekle et al., 2005).

Different cell types have various thresholds for electroporation (typically from 0.5 to 1 V). When the magnitude of an electric field is greater than the threshold for a given cell, the high voltage electrical pulses can lead to cell membrane disruption through the formation of small defects and transient aqueous pores that consequently affect cell structure, processes, and signaling (Figure 3). These events can occur in all mammalian cells and may exist for a period of time in the order of minutes. When the applied electric field is moderate and the pulse duration is limited, the cell membrane can recover

from the poration state and survive.

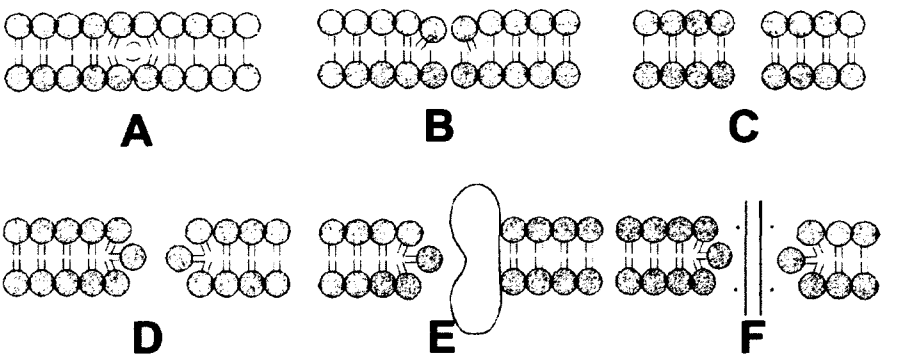

Figure 3. Hypothetical structural rearrangements of bilayer membrane (Weaver, 1993) (redrawn by Yiling Chen)
(A) Free volume created allowing entry of uncharged molecules (Potts and Francoeur, 1990).
(B) Dimple on one layer (local membrane compression and thinning).
(C) Formation of hydrophobic pore, a precursor of hydrophilic pore (Weaver and Chizmadzhev, 1996) and a possible route for water transport (Abiror et al., 1979; Jansen and Blume, 1995).
(D) A complete hydrophilic pore.
(E) Composite pore involving a membrane protein (Weaver, 1993).
(F) Interaction between the inserted long, charged molecule and hydrophilic pore (Weaver, 1993).

The conventional electroporation process utilizes an electric field of 0.1 to 1 kV/cm magnitude to reach the required voltage across the membrane with a duration time greater than ~100 μs (Mir, 2001; Weaver, 2003). Under these conditions, the plasma membrane can reseal from poration within a 5 min post-application time frame (Kolb et al., 2006). The electroporation and resealing procedure is widely used in molecular biology and biotechnology experiments and has been implemented for drug delivery (Golzio et al., 2002; Harrison et al., 1998; Lee et al., 1992; Lundqvist et al., 1998; Mir et al., 1995; Neumann et al., 1996; Neumann et al., 1982). Electroporation and subsequent permeabilization of the plasma membrane can lead to the release of ions and small

molecules from the cell (Mir, 2001), as well as enable delivery of molecules into the cell such as fluorescent markers (Bartoletti et al., 1989; Gift and Weaver, 2000; Prausnitz et al., 1993), anticancer drugs such as bleomycin (Mir et al., 1991), and large molecular proteins (Berglund and Starkey, 1989; Graziadei et al., 1991; Lukas et al., 1994; Rols et al., 1998; Uno et al., 1988; Verspohl et al., 1997) and DNA (Heller et al., 1996; Titomirov et al., 1991).

One major advantage of conventional electroporation is that this method is not restricted to particular cell types; thereby, increasing its applicability in several fields. However, excessive electroporation with a very high electric field, extended pulse duration and recurrent pulses may result in complete membrane permeabilization which can lead to non-thermal necrotic cell death (Davalos et al., 2005; Gift and Weaver, 2000; Keese et al., 2004; Sersa et al., 1994).

Thus, parameters of the applied electric field such as field strength, pulse duration, number of pulses, shape of the wave form, etc. greatly affect the degree of membrane electroporation, with downstream effects on molecular release or uptake and cell survival. Due to fortified cellular walls, bacteria are capable of tolerating long-duration pulses with millisecond ranges. Conversely, eukaryotic cells such as mammalian cells and isolated plant or yeast protoplasts are more vulnerable to electric fields and therefore shorter pulses and lower electric fields are required to avoid irreversible membrane breakdown and lysis of these cell types (Zimmermann, 1996). Thus, with shorter pulses of 10–100 μs duration, the survival rate of pulse-treated mammalian cells of various cell lines are substantially improved (Diederich et al., 1998). This suggests that using ultra-short pulses of sub-microsecond durations could further reduce the effect of the electric field

and improve the survival of eukaryotic cells after a desired treatment regimen. However, earlier conventional pulse generators and even commercial devices were not able to produce sub-microsecond pulses of field strengths sufficient for electroporation of cell membranes.

1.4 Nanosecond Pulse Effect on Membrane

Recently, technological advances in electroporation have significantly improved the ability to produce square or trapezoidal pulses with much shorter durations (1–300 ns) and higher electric fields (up to 300 kV/cm) (Schoenbach et al., 2004). Based on the duration of this short pulse, the electric field is often called a nanosecond pulsed electric field (nsPEF). Since the pulse duration is shorter than the plasma membrane charging time, effects on plasma membranes will decrease and intracellular effects predominate. Thus, the cell response is predicted to change significantly compared to classical plasma membrane electroporation, and formation of smaller, short-lived nanopores with nsPEFs are suggested (Beebe et al., 2002; Beebe et al., 2003).

The effects of nsPEFs on mammalian cells have only recently been explored (Beebe et al., 2002; Beebe et al., 2003). Such pulses can cause apoptosis, cytochrome-*c* release, caspase activation, phosphatidylserine (PS) translocation, disruption of nuclear DNA, conformational changes of membrane bound proteins and/or DNA-chromatin complexes (Beebe et al., 2003; Joshi et al., 2002), small and delayed amounts of propidium iodide (PI) transport across the plasma membrane (Beebe et al., 2002; Deng et al., 2003), and calcium uptake into subcellular granules (Beebe et al., 2002; Schoenbach et al., 2001; Schoenbach et al., 2007; Vernier et al., 2003).

Although the applied fields are extremely strong (up to 300 kV/cm) with field intensities several hundreds of times higher than electroporation pulses, their effects on cells and tissues are non-thermal due to the short pulse duration (nanoseconds) and low energy. This has created new opportunities for research that focuses on cellular responses due primarily to intracellular electro-effects (Beebe et al., 2003; Buescher and Schoenbach, 2003; Schoenbach et al., 2001). The ability of the nsPEF method to induce apoptosis of biological cells also offers a promising new therapeutic strategy to treat cancer (Beebe et al., 2002; Nuccitelli et al., 2006). Based on known effects of electric fields on cells (Weaver, 2000), this phenomenon may be due to membrane charging effects, possibly with 'electrical breakdown' or nano-electroporation effects on subcellular membranes (Joshi et al., 2002).

Unlike conventional electroporation, nanosecond electrical pulses (nsEPs) do not trigger the uptake of membrane integrity marker dyes, such as propidium iodide and trypan blue (Pakhomov et al., 2007b; Thomas Vernier et al., 2004; Vernier et al., 2003). With a size around 2 nm, trypan blue is not able to pass through pores opened by nsEPs on the cell membrane because those pores have a suggested maximum size of about 1–1.5 nm (Pakhomov et al., 2009). The probability of pores forming in the membrane is not a linear relationship with the transmembrane voltage as suggested by recent molecular dynamics simulations of pore formation (Tieleman, 2004). Resealing of the pores takes as long as several minutes, indicated by the recovery of membrane conductivity, which is comparable to electroporation (Pakhomov et al., 2007a). The major parameters responsible for the pulsed electric field effects are pulse duration and field magnitude. In addition, the conductivity of the medium in which cells are suspended is an important

factor. Later changes on membrane integrity and secondary cell responses depend on complex interactions of biophysical and biochemical processes.

Because of the short pulse duration (nanoseconds), the nsPEF may affect intracellular structures (membranes) and functions (cell signaling) with fewer responses in the outer plasma membrane. Although biological effects on the plasma membrane, such as phosphatidylserine (PS) externalization associated with apoptosis can be measured, this PS externalization can also result from direct electric field effects. Examinations of plasma membrane integrity following electric field treatments using fluorophores and/or molecular probes are generally impossible due to their large size. Although recent computational studies (models) have suggested nanopores and nanochannels for phosphatidylserine externalization (Hu et al., 2005), the physical proof for nsPEFs effects on membrane embedded proteins and ion channels is not yet clear.

As stated earlier, the actual biological effects produced with electric field are closely associated with the experimental conditions, such as pulse number, pulse duration, field strength (Beebe et al., 2003; Deng et al., 2003) and the cell type (Beebe et al., 2003; Hair et al., 2003; Stacey et al., 2003). When the pulse frequencies are low compared with the inverse of the charging time of the plasma membrane (β–frequency) (Schoenbach et al., 2001), the voltage across the plasma membrane is similar to the voltage drop across the entire cell, and the plasma membrane will incur damages (electroporation) while leaving the cell interior protected. However, for high pulse frequencies, the voltage across the outer membrane decreases and the applied electric field increases across the cytoplasm. Therefore, the outer membrane becomes transparent for high-frequency electric fields and the cell interior becomes exposed to the applied electric field. With

high electric field and short pulse durations that are less than the charging time of the cell membrane, the electric field has an increased probability of accessing and interacting with intracellular structures (Beebe et al., 2003; Nuccitelli et al., 2006). Experimental studies have demonstrated that nsPEFs can induce damage to intracellular granules in human blood eosinophils, while the cell outer membranes still maintain their integrity (Schoenbach et al., 2004). This illustrates the possibility to manipulate intracellular effects with electric fields similar to conventional electroporation of the outer membrane.

Although the effects of high frequency electroporation are well known (Schwan, 1968), few studies have been conducted to investigate intracellular effects, e.g., the electroporation of intracellular membranes. This is partially due to the aforementioned technical difficulty of generating large intracellular electric fields. Assuming that electroporation of intracellular membranes (intracellular electro-manipulation) requires potential differences across such membranes in the order of 1 V, electric fields as high as 10 kV/cm will be needed for poration of intracellular structures with characteristic dimensions of 1 μm.

The advancement of technology for generating high voltage, short duration pulses has enabled many theoretical and experimental studies to be conducted with nsPEFs. However, none have demonstrated the physical damages that are proposed to occur to either the plasma membrane or the membranes of the intracellular organelles. In this study, we present the direct morphological and chemical evidence of cell response to electric pulses. To evaluate the effect of nanosecond pulses on cell morphology, this research utilizes the standard experimental procedure of nsPEF employed in prior apoptosis studies. Specifically, 1 to 5 pulses of 60 ns and 300 ns duration (each pulse)

under an electric field of 60 kV/cm was used and the effects were evaluated. In addition, a typical microsecond regimen, as used in electroporation (2 to 6 pulses of 100 μs duration each under an electric field of 1.2 kV/cm), was performed.

To investigate the associated changes (e.g. cell membrane permeability with nanosecond and microsecond pulses), a trypan blue uptake test was performed immediately after pulse to differentiate membrane damaged or dead cells from intact cells. With a long-term (24 hrs) incubation of cells after pulse(s), we were able to examine the pulse effects on cell viability. Along with the morphological observations on the subcellular organelle (mitochondria), its function, which is represented by mitochondria membrane potential, was monitored by JC-1 fluorescent dye.

CHAPTER 2

MATERIAL AND METHODS

2.1 Cell Culture

Murine melanoma B16-F10 cells were obtained from ATCC (Manassas, VA) and stored frozen in liquid nitrogen until needed. Cells were thawed in 37 °C water bath and then transferred to a 75 mL culture flask containing Dulbecco's modified Eagle's medium (DMEM) supplemented with 10% fetal bovine serum (FBS, Atlanta Biologicals, Lawrenceville, GA), 4 mM L-Glutamine (Mediatech, Cellgro Herndon, VA), and 2% Penicillin–Streptomycin solution (Mediatech, Cellgro Herndon, VA). The cells were grown in a humidified incubator at 37 °C with 5% CO_2, and maintained in the exponential growth phase by sub-culturing three times a week.

Prior to each experiment, the culture medium was removed and discarded. The cell layer was briefly rinsed with Hank's balanced salt solution without Ca^{2+} or Mg^{2+} (HBSS) (Mediatech, Cellgro Herndon, VA), followed by the addition of 2.0 mL of trypsin-EDTA solution. Cells were examined under an inverted microscope until the cell layer was disrupted after 5 min. Six mL of complete growth medium was then added to the flask and the cells were aspirated by gently pipetting. The cells were washed 1–2 times with cell medium 10 min before electrical pulsing. For electrical pulse experiments, B16-F10 cells were maintained at a concentration of 1×10^6 cells per 150 μL in Hank's balanced salt solution (HBSS) without Ca^{2+} or Mg^{2+}.

2.2 Pulse Generators

The pulse generator is a piece of electronic test equipment which is used to generate pulses. In this study, two nanosecond pulse durations (60 and 300 ns) with amplitude of 6 kV were employed, and the durations were controlled by cables' length of transmission line type pulse generator. The pulse forming line acts as a capacitor and the capacitance is proportional to the cable length, i.e. longer cables have larger capacitance and can therefore deliver pulses with longer duration. The charges are released once they are connected to the biological target by a high voltage switch. The moving charges form an electric current and create a voltage pulse across the biological load, which can be understood as a resistance. The 60 ns pulse generator included five parallel high voltage 50 Ω cables, which achieved a 10 Ω impedance required for matching the resistance of the suspension in the cuvettes. The design of the 300 ns pulse generator was similar to the 60 ns generator; however, for the 300 ns pulse the length of the five parallel cables was increased by 5× that of the 60 ns system (Figure 4A). Each cable still has an impedance of 50 Ω (the characteristic impedance of coaxial cable which is independent to length), and the resulting total impedance of the network containing five parallel cables is therefore 10 Ω. Thus, the pulse duration is proportional only to the length of the cable, i.e. the capability of storing charges.

A BTX T820 DC generator (BTX, San Diego, CA) was used to generate rectangular direct current micro-second pulses. This electric device is able to deliver pulse duration from 1 μs to 99 ms and the pulse number can be chosen from a range of 1-99 depending on the voltage and pulse length settings. The electric field strength was

maintained at 1.2 kV/cm by adjusting the output voltage (120 V) of the generator and each pulse duration was maintained at 100 μs.

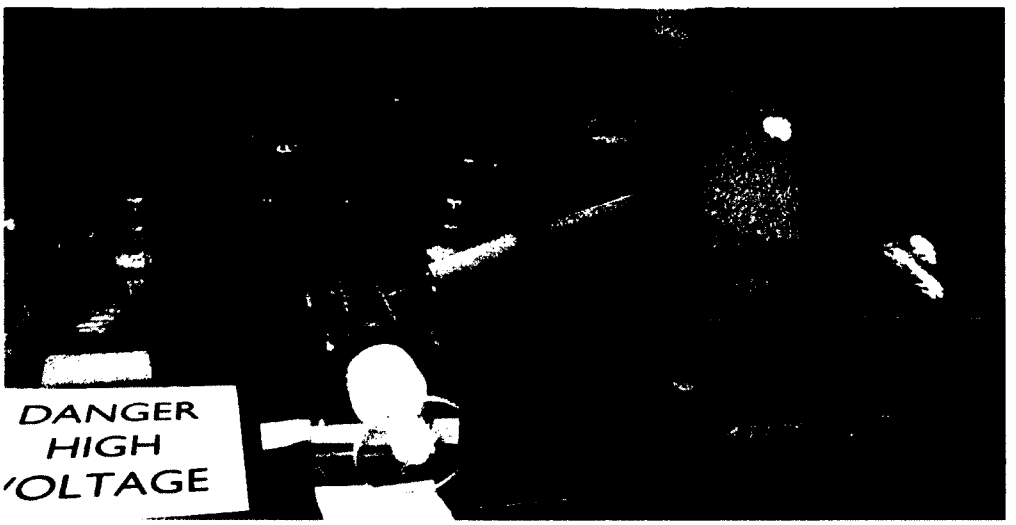

Figure 4. Devices used for electric pulses
(A) Experimental setup. The pulse station is connected to the electrode system and the voltage control is adjusted by transmission line. Arrow refers to one electrode.
(B) The electroporation pulser cuvettes with a 0.1mm gap.
(C) A typical single pulse wave monitored by oscilloscope.

The voltage across the object (cell samples) was monitored using a high voltage probe (P6015A, Tektronix, Beaverton, CA), and the current was measured by means of a Pearson coil (model 2877, Pearson Electronics Inc., Palo Alto, CA). Current and voltage were recorded simultaneously using a digitizing oscilloscope (Figure 4C) (TDS3052, Tektronix, Beaverto). The pulse frequency (1.0± 0.5 Hz) was also monitored from the oscilloscope at the same time.

2.3 Electric-Field Exposure

After the cells were harvested, they were centrifuged and re-suspended in HBSS at a concentration of 1×10^6 cells/mL, which was monitored by a hemocytometer. Using the hemocytometer, the cell suspension was then concentrated and an aliquot of 150 μL (containing 1×10^6 cells) was pipetted into the electrode gap of a standard electroporation cuvette (Biosmith, San Diego, CA) (Figure 4B). The rectangular pulses were applied across the parallel electrode plates of the cuvette with a 0.1 cm electrode gap, providing a homogeneous constant electric field. The cuvette in the pulse generator was exposed to 1–5 rectangular pulses of 60 or 300 ns duration with amplitudes of 60 kV/cm applied at about 1.0 Hz (± 0.5 Hz). Pulse shape, duration, and amplitude were monitored throughout each exposure on a digital oscilloscope (Tektronix, TDS3052B, Wilsonville, OR) with a high-voltage probe (Tektronix, P6015A, Wilsonville, OR). Similar exposures (2–6 pulses) were applied for a microsecond duration (100 μs) under electric field of 1.2 kV/cm. The control group of each pulse condition followed the same procedure of that group except without any applied pulse(s). For the pulsed treated groups, the energy density (W) deposited on membrane can be calculated by:

$$W= \sigma_M E_M^2 \tau \qquad (2)$$

Here W is energy density, σ_M is membrane conductivity, E_M is electric field in the membrane and τ is charging time.

Due to high voltage used in this study, special cautions are required for conducting the pulsing experiments. The Frank Reidy Research Center for Bioelectrics provides a course to guide the safe use of high voltage pulse power equipment and the author have been trained in the safe use of the equipment.

2.4 Transmission Electron Microscopy

Morphological effects were examined using transmission electron microscopy (TEM). TEM was chosen as it allowed for direct morphological observations from high-quality and high-resolution images (Erni et al., 2009). In contrast with the light microscope, TEM utilizes an electron beam that passes through the specimen prepared as an ultra-thin layer, interacting with the specimen as it passes through. An image is formed from the interaction of the electrons transmitted through the specimen. The image is magnified and focused onto an imaging device.

For TEM analysis, each sample after pulse treatment was immediately transferred to the fixation process. A mixture of 2.5% glutaraldehyde, 2% paraformaldehyde, 0.15 M sucrose buffer and 0.1 M sodium cacodylate (Electron Microscopy Sciences, Hatfield, PA), which had a final pH of 7.4, was added to each sample immediately after the pulse(s). The fixation solution was kept at 4 °C for 1 hr. Following fixation, samples were rinsed with sodium cacodylate buffer 3× for 10 min each. Samples were then incubated with 1% osmium tetroxide (Electron Microscopy Sciences, Hatfield, PA) for 2 hrs at room temperature, followed by repeated washes with sodium cacodylate buffer. Dehydration of samples was achieved by washing with 25% ethanol (Electron Microscopy Sciences, Hatfield, PA) 15 min, 50% ethanol with 2% uranyl acetate for 1 hr, 75% and 95% ethanol for 15 min 1×, followed by a 100% ethanol wash 2× for 15 min each. Finally, samples were washed 2× with 100% propylene oxide (PO; Electron Microscopy Sciences, Hatfield, PA) for 15 min each.

For the sample infiltration and embedding steps, all procedures were carried out

on a rotating mixer. Infiltration was performed stepwise with 30% Embed 812 resin with PO for 1 hr at room temperature, followed by incubation with 70% resin with PO for 4 hrs at 4 °C and finally 100% resin overnight. Polymerization of the samples was achieved by incubation at 60 °C for 48 hrs. Ultrathin sections were cut with an ultramicrotome (RMC, 1T2C, Boeckeler Instruments, Inc. Tucson, Arizona) equipped with diamond knife (DDK, Delaware Diamond Knives, Wilmington, DE), and mounted on a copper grid (Electron Microscopy Sciences, Hatfield, PA). Ultrathin sections was then stained with Reynolds lead citrate (Electron Microscopy Sciences, Hatfield, PA) and examined with a JEOL 1200EXII transmission electron microscope (Jeol, Tokyo, Japan).

2.5 Trypan Blue Uptake Test Immediately After Pulse

Trypan blue dye is used to differentiate damaged cells from healthy cells in suspension. Intact cell membranes of live cells will exclude trypan blue, whereas dead or membrane disrupted cells will readily take up this dye (Strober, 1997). To perform the uptake test, the cell suspension is mixed with trypan blue followed by visual inspection under the microscope to determine whether cells take up or exclude trypan blue. The viable cells will have a clear cytoplasm while unhealthy cells will have a blue or bluish cytoplasm.

Control and pulsed cells were removed with their media from each cuvette and mixed 1:1 with a volume of 0.4% trypan blue (Sigma St. Louis, MO) for 3 min after pulsing. A small volume of this mixture was then placed on a hemocytometer. The cells were then counted as either stained or unstained and the percentage of trypan blue uptake can be calculated using Eq. 3:

$$\text{Trypan blue uptake (\%)} = \frac{\text{Total number of stained cells in the aliquot}}{\text{Total number of all cells in the aliquot}} \times 100\% \qquad (3)$$

At least 150 cells were counted in each experimental group. The same amount of cells was also used in the analysis of long-term cell viability analysis.

2.6 Long-Term Cell Viability Assay

Another set of pulsed cells were removed from cuvette and returned to the culture for the long-term test. These cells were removed from the cuvette immediately after the pulse(s) and placed in six-well plates and cultured as describe earlier. After 24 hrs, cells were trypsinized and the cell suspension was centrifuged for 3 min at 1000 ×g and the supernatant discarded. The cell suspension was then mixed with 0.4% trypan blue in a 1:1 ratio and incubated at room temperature for 3 min. Following incubation, the B16-F10 cells were examined and quantified for viability in a hemocytometer and calculated as below:

$$\text{Viable cells (\%)} = \frac{\text{Total number of viable cells in the aliquot}}{\text{Total number of all cells in the aliquot}} \times 100\% \qquad (4)$$

2.7 Mitochondrial Potential Analysis

In this study, mitochondrial membrane potential was monitored by a cationic dye JC-1 (JC-1, Sigma, St. Louis, MO). A mitochondrial membrane potential disrupter, CCCP (carbonyl cyanide 3-chlorophenylhydrazone) (Sigma, St. Louis, MO), which can fully disrupt inner mitochondrial membrane potential, was used as a positive control. JC-1 exhibits potential-dependent accumulation in mitochondria, which can be seen by a fluorescent emission shift from green to red, where the two colors are the approximate emission peaks of monomeric (~529 nm) and aggregate forms (~590 nm) of JC-1,

respectively (Smiley et al., 1991). In healthy cells with high mitochondrial potential ($\Delta\psi m$), JC-1 spontaneously forms complexes known as J-aggregates with intense red fluorescence. In apoptotic or unhealthy cells with low $\Delta\psi m$, JC-1 remains in the monomeric form, which shows only green fluorescence.

The formation of J-aggregates is concentration dependent (Di Lisa et al., 1995; Hibino et al., 1991; Reers et al., 1991) and the resulting color shift has been demonstrated in earlier studies of different cell types, such as myocytes (Di Lisa et al., 1995) and neurons (White and Reynolds, 1996). JC-1 can also be applied to intact tissues (Sick and Perez-Pinzon, 1999) and isolated mitochondria (White and Reynolds, 1996). The advantage of JC-1 is the affinity of this probe for mitochondrial membranes as opposed to plasma membranes and its sensitivity and consistency in measuring membrane potential changes compared with other cationic dyes such as $DiOC_6$ (Di Lisa et al., 1995) and rhodamine 123 (Mancini et al., 1997). Therefore, JC-1 is commonly applied for detection of the mitochondrial potential changes accompanied with the apoptosis process (Kulkarni et al., 1998; Mancini et al., 1997; Wadia et al., 1998).

As an ideal indicator for membrane potential, changes in the ratio of green to red fluorescence are solely dependent on the monitored property, i.e. mitochondrial membrane potential. Other factors such as mitochondrial size, shape, and density have no effect on the fluorescent pattern. Using repetitive fluorescence ratio detection allows us to compare measurements of membrane potential and determine the percentage of mitochondria within a population that respond to the applied stimulus, i.e. electric pulses in this study (Smiley et al., 1991; White and Reynolds, 1996).

As a control, cells were incubated with 1 μL of 50 mM CCCP (carbonyl cyanide 3-chlorophenylhydrazone, Sigma St. Louis, MO) at 37 °C for 5 min, followed by addition of 10 μL of 200 μM JC-1 (2 μM final concentration) with a second incubation at 37 °C, 5% CO_2 for 30 min. The cells were then washed 1× with 2 mL of warm phosphate-buffered saline (PBS) added to each tube. The cells were pelleted by centrifugation and then re-suspended with 500 μL PBS by gently flicking the tubes.

2.8 Flow Cytometry

Cells were removed from cuvettes (1×10^6 cells/150 μL) that were either exposed or not exposed to the electric pulses and incubated with JC-1 for 20 min. Diluted cell suspensions (1×10^6 cells/mL) were then analyzed by using a Becton-Dickinson FACS Calibur flow cytometer (Sparks, MD). Cells were prepared at around 10,000 per sample and each sample was excited under a 488 nm argon laser and evaluated by determining their position on a forward-scatter versus side-scatter contour plot. Cells were selected and gated based on normal forward- and side-scatter characteristics observed on a scatter plot (FSC versus SSC). Fluorescent emissions (green and red) were detected in FL-1 and FL-2 channels respectively. These two detectors have corresponding bandpass filters of 515 – 545 nm and 564 – 606 nm, which allow green and red fluorescence to pass through separately. Data was stored and analyzed with FlowJo 7.2.5 software (include reference or company location).

2.9 Statistical Analysis

In this study, all experiments were completed with at least 3 replicated runs. The data presented here was the average value from multiple runs under each condition and the standard deviation has also been provided. To compare the significance between pulse-treated and control group, the data was analyzed by using the Statistical Package for Social Sciences (SPSS) 19.0 program. The percentage of trypan blue uptake, long term cell viability after pulse(s), and mitochondrial irregularity were evaluated by one-way Analysis of Variance (ANOVA) and followed by Dunnett post-hoc test. Because the mitochondria membrane potential drop data was not a normal distribution, it was arcsine-transformed. The mitochondria membrane potential drop (J-aggregates) was tested with one-way ANOVA after transformation. In all ANOVA analysis, a P value ≤ 0.05 was considered to be statistically significant.

CHAPTER 3

RESULTS

3.1 Cell Membrane Changes

3.1.1 Morphological Changes under Transmission Electron Microscopy

To investigate the physical changes hypothesized to occur to either the plasma membrane or the membrane of intracellular organelles following the application of high-voltage (HV) electric pulses, melanoma B16-F10 cells were treated with two types of HV electric pulses. The higher electric field (60 kV/cm), using 6 kV over a 0.1 cm gap, was applied to cells in suspension with two different nanosecond scale durations (60 and 300 ns). The lower electric field had strength of 1.2 kV/cm (120 V over a 0.1 cm gap) and was conducted with duration of 100 μs. Different pulse numbers (1 to 6 pulses) were applied to the three pulse conditions and three replicated experiments were performed for each pulse number. Immediately after pulsing, chemical fixatives were added and the morphological changes of B16-F10 cells were investigated by TEM.

B16-F10 mouse melanoma cells are about 10~15 μm in diameter and morphological observations were carried out on both the exterior and interior of the cell. Figure 5 illustrates cells of the control group and treatment groups using the 60 ns, 60 kV/cm pulse condition. B16-F10 cell membranes and nuclear envelopes in the control group maintained their lipid bilayer integrity and subcellular organelles have a regular appearance in terms of size and shape. The treatment groups with only 1-2 pulses (image

not shown) also demonstrated normal morphology. With 3 pulses, cell membranes maintained a normal morphology, while swollen mitochondria were observed primarily in the exhibition of decreased and disorganized cristae.

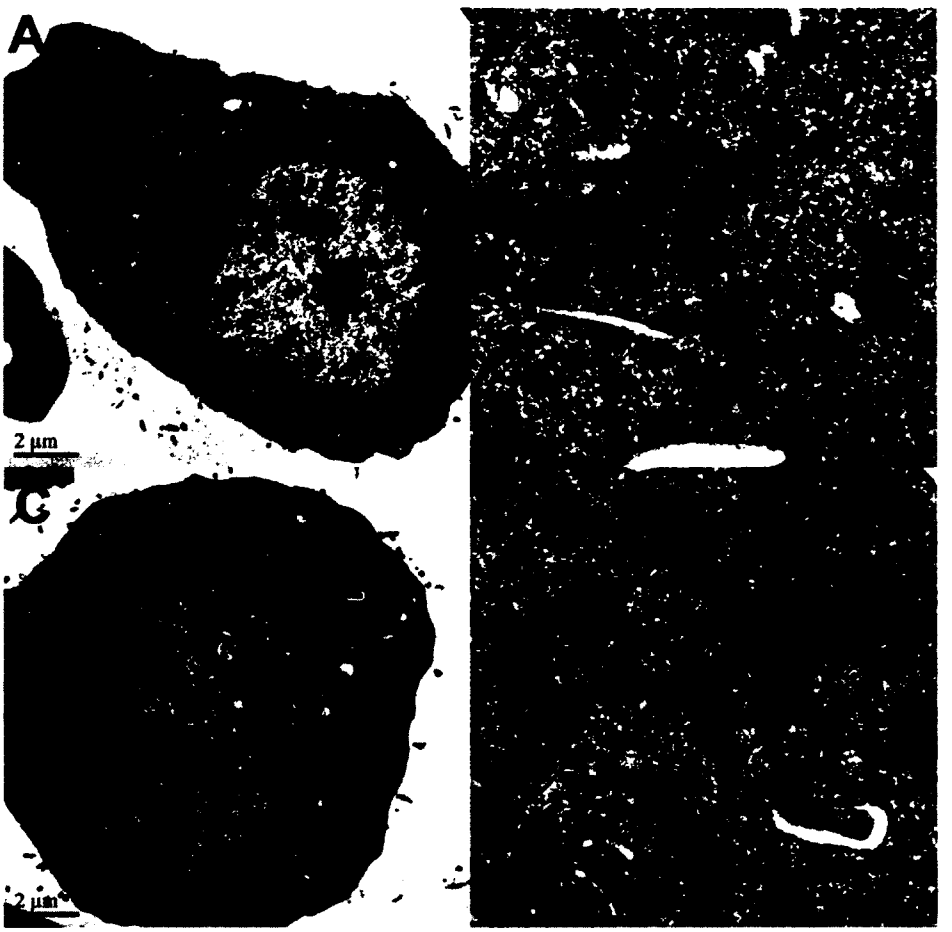

Figure 5. TEM images showing cells treated with 60ns 60kV/cm pulse conditions (A-B) Control melanoma B16-F10 cells without pulsing at 6K and 40K magnification receptively. The arrows in figure B refer to healthy mitochondria.
(C-D) Cells treated with 3 pulses of 60 kV/cm 60 ns duration at 6K and 40K magnification receptively. Mitochondria which exhibited swollen and cristae loss are pointed with arrows.

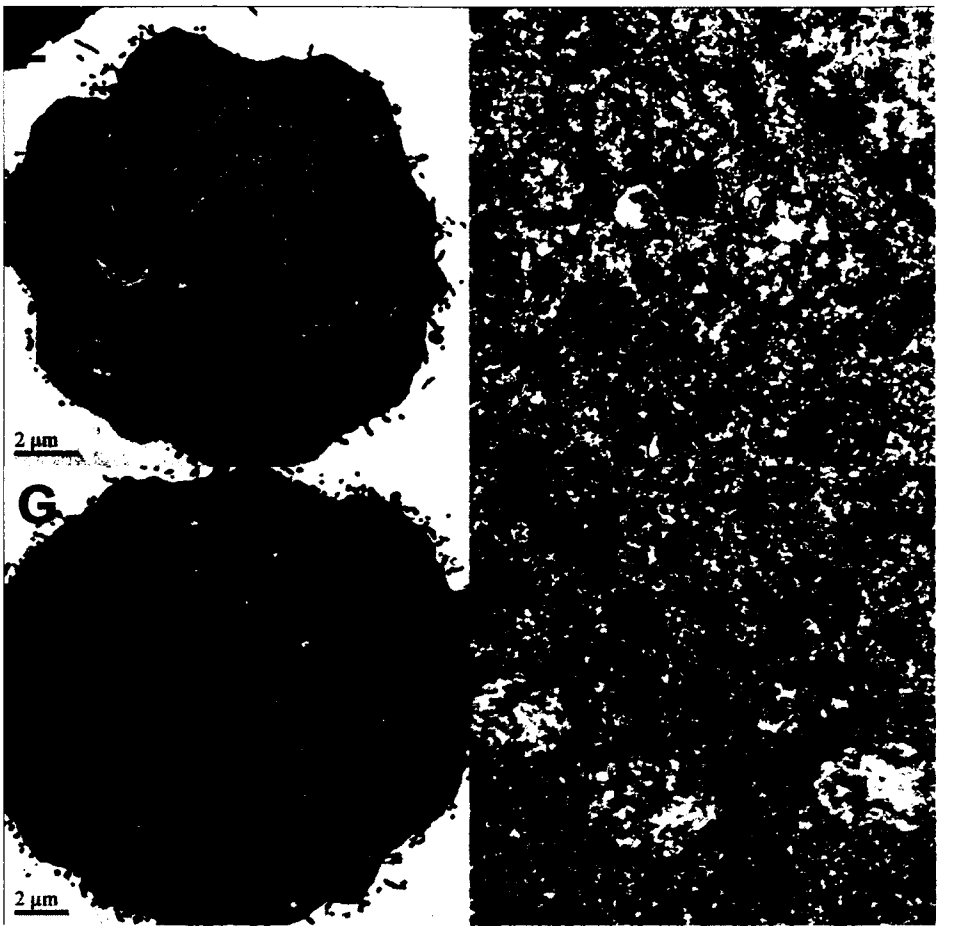

Figure 5 (Continued). TEM images of cells treated with 60ns, 60kV/cm pulse condition (E-F) Cells with 4 pulses at a magnification of 6K and 40K respectively. Mitochondria with swollen appearance and cristae loss are indicated by arrows.
(G-H) Cells with 5 pulses at 15K and 40K magnification respectively. Arrows point toward mitochondria which exhibit loss of cristae.

Following 4 pulses under the same pulse condition, cell membranes exhibited no surface changes; however the internal mitochondrial membranes showed a totally disorganized structure. With further increased pulse number (5 pulses), the morphology of cellular membrane remained normal but the mitochondria exhibited increased cristae loss. In total after 5 pulses, approximately 62% of the mitochondria demonstrated

irregular morphology, which included missing cristae and structural disorganization. Such a high percentage of irregular mitochondria inside the cell suggested large effects under 60 ns, 60 kV/cm pulse condition with 5 pulses.

Under the same electric field (60 kV/cm), but with a longer pulse duration (300 ns), similar effects were observed as compared to the 60 ns duration pulses (Figure 6). The control group and treated groups with 1-2 pulses exhibited normal cell membrane, nuclear envelope, and mitochondrial morphology. Irregular mitochondria became observable with 3 pulses and mitochondria displayed clear cristae destruction with 4 or more pulses. Under higher magnification (×40K), mitochondria with 5 pulses (Figure 6F) exhibited complete cristae loss in contrast to cells with fewer pulses (3 pulses, Figure 6C) where cristae damage was less significant. This suggested increased mitochondrial disfunction with an increased number of electric pulses.

With the lower electric field (1.2 kV/cm), microsecond scale (100 μs) pulse condition, we found that mitochondria appeared healthy and normal following 5-6 pulses compared with the control group (Figure 7). With 5 microsecond pulses, mitochondria cristae structures remained clearly visible under high magnification (×40K) (Figure 7B). This was in sharp contrast to nanosecond pulses where cristae destruction was observed. For other membrane structures, the control B16-F10 cell membranes and nuclear envelopes retained their integrity and cell organelles had a normal appearance. Following 6 pulses, mitochondria maintained normal morphology but filopodial projections could be occasionally found on cell membrane after the 6-fold electroporation pulsing (Figure 7 C-D).

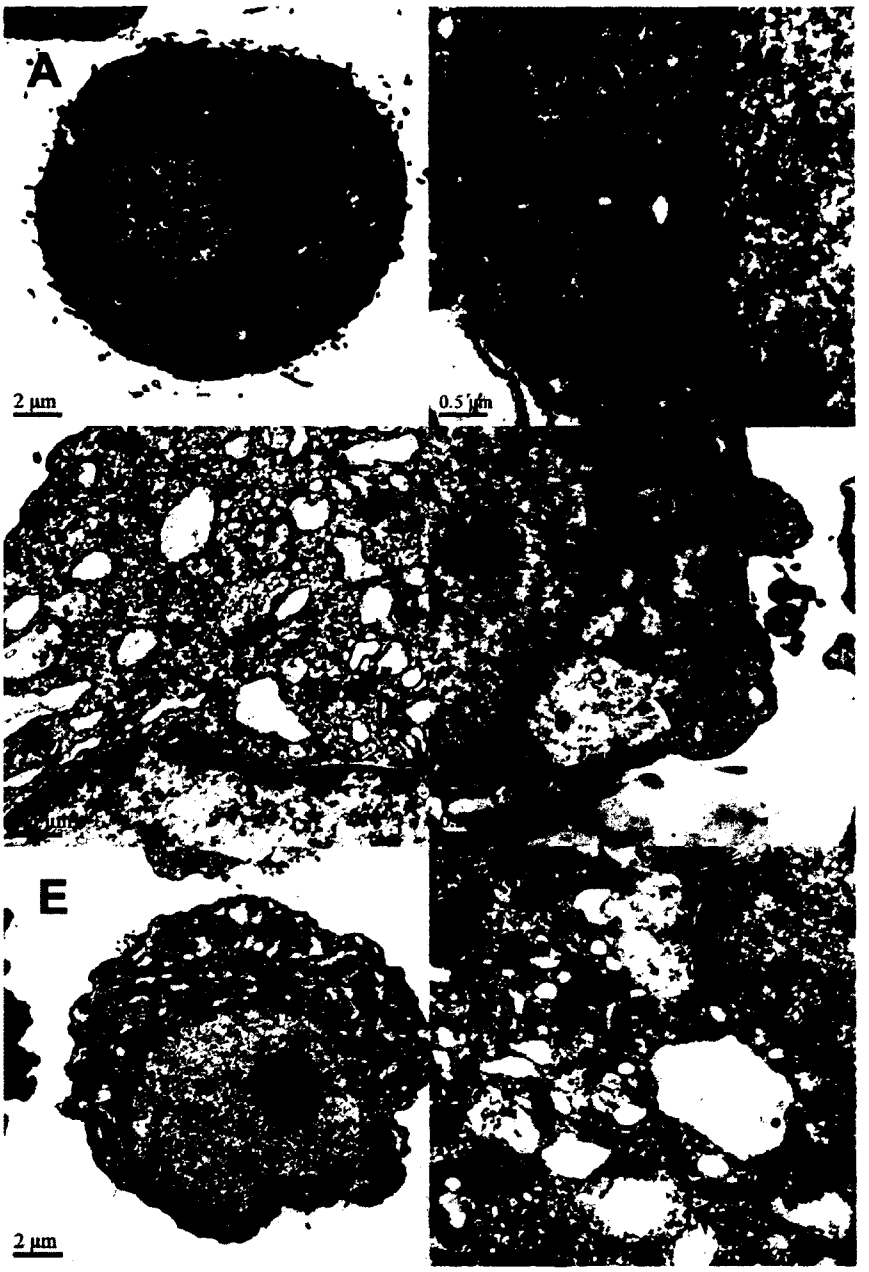

Figure 6. TEM images for the control group and treatment groups following application of the 300 ns, 60 kV/cm pulse condition. Arrows point toward swollen mitochondria which contain cristae loss
(A) Control melanoma B16-F10 cells without pulsing at 6K magnification.
(B-D) Cells treated with 2, 3, and 4 pulses, at 10K, 40K, and 40K magnification respectively.
(E-F) Cells treated with 5 pulses at 6K and 40K magnification.

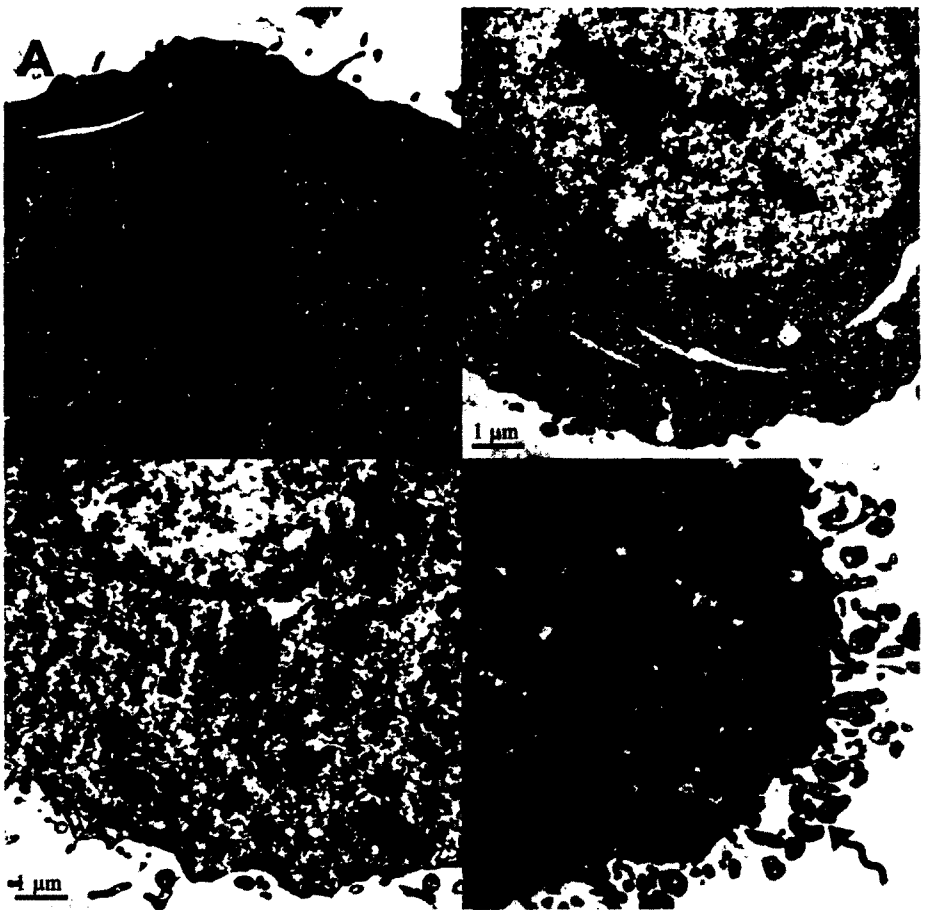

Figure 7. TEM images of control group and pulse treated cells under 1.2 kV/cm electric field and 100 μs duration
(A) Control melanoma B16-F10 cells without pulsing at 15K magnification.
(B) Melanoma B16-F10 cell treated with 5 pulses at 15K magnification. Arrow refers to a healthy mitochondrion.
(C) Melanoma B16-F10 cell treated with 6 pulses at 15K magnification. Healthy mitochondria are labeled with straight arrow.
(D) Melanoma B16-F10 cell treated with 6 pulses at 15K magnification. Filopodia are labeled with curved arrow.

The filopodia phenomenon under microsecond pulses suggests some cell membrane changes, which may be comparable to electroporation. Other experimental studies using melanoma B16-F10 cells showed 90% trypan blue uptake at approximately

6 pulses with single square-waves at an amplitude of 1.2 kV/cm and durations of 100 μs (Beebe et al., 2002). Conversely, there were no pore-like structures observed under nanosecond pulse conditions. Other experimental and modeling evidence (Chen et al., 2007; Schoenbach et al., 2001; Tekle et al., 2005; Wang et al., 2009; White et al., 2004) indicated that nsPEFs induce "nanopores" about 1-1.5 nm in diameter in all cell membranes while conventional electroporation induced large pores in the plasma membranes. However, neither large nor small pores were visible with the current TEM photos, which had a post-pulse fixation time less than 10 min.

3.1.2 Trypan Blue Uptake Analysis

Based on an electric model of biological cells (Schoenbach et al., 2001), it was predicted if the pulse duration was longer than charging time, it would have more effects on the plasma membrane. To test this hypothesis directly, melanoma B16-F10 cells were exposed to pulsed electric fields with different durations (60 ns, 300ns, and 100 μs) and varied number of the pulses. Effect of cell membrane perturbation was examined by trypan blue uptake following pulse treatment. Trypan blue labeling was based on the fact that the chromophore is negatively charged and cannot enter the cell unless the membrane is damaged. If the cell membrane response correlates with electric pulses, the level of trypan blue uptake, which is an indication of plasma membrane integrity, is expected to increase as the pulse duration or the pulse number, is increased. To compare the effects of nsPEF and classical electroporation on plasma membrane integrity, B16-F10 cells were also exposed to 100 μs pulses at 1.2 kV/cm, which was a traditional electroporation condition.

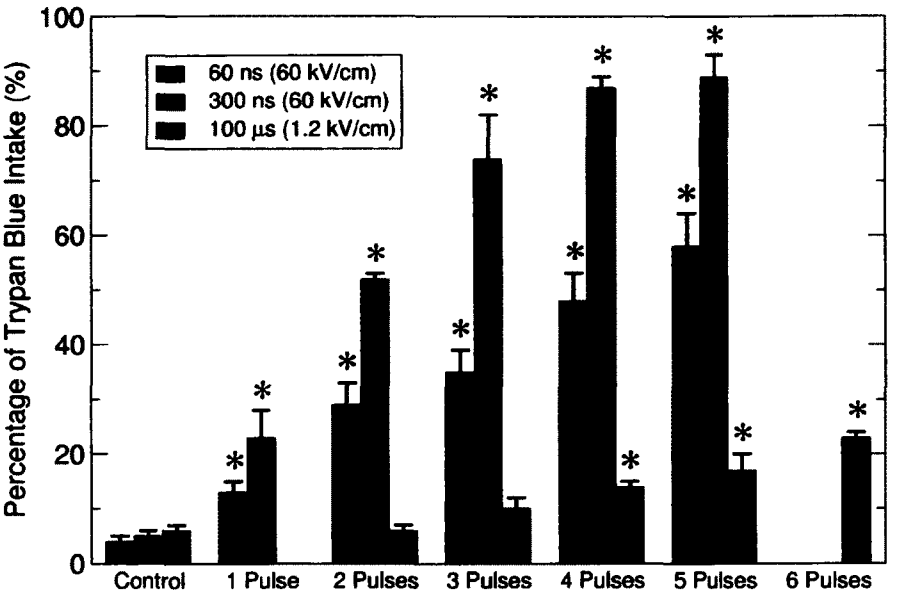

Figure 8. Percentage of trypan blue uptake following pulse treatment
Pulse durations of 60 ns, 300 ns, and 100 µs are shown in red, blue, and green respectively. Each bar represents the mean ± standard deviation of three replicated experiments. Significance compared with control group ($P \leq 0.05$) by one factor ANOVA and followed by Dunnett test is indicated with asterisk (*) above the error bar.

In this study, trypan blue was added to pulse-treated melanoma B16-F10 cells for 5 min directly following pulse application. For different pulse conditions, all treatment groups exhibited a steady increase in trypan blue uptake that corresponded to the increase of the pulse number (Figure 8). The largest amount of trypan blue uptake was found for the 300 ns (60 kV/cm) pulse treated group. From the control to the group with 3 pulses, each additional pulse introduction resulted in more than a 20% increase in trypan blue uptake as compared with the previous group. Trypan blue uptake for groups with 4 and 5 pulses reached a saturation of around 90%.

Trypan blue uptake for cells treated with 100 µs (1.2 kV/cm) was not significantly different from the control with 2 and 3 pulses and relatively low for 4-6 pulses,

suggesting a less perturbed cell membrane under μs pulsing condition. This is consistent with TEM images which showed minimal effects on plasma membrane integrity with the 100 μs pulses. In comparison, pulse treated cells which were under the 60 and 300 ns durations began to show significant differences from the control with the first applied pulse.

3.2 Sub-Cellular Changes

3.2.1 Mitochondria Irregularity Changes

The morphology of mitochondria was examined using TEM. With different pulse conditions, mitochondria might exhibit various changes which include cristae missing, size decrease and disorganization and outer membrane distortion. The total mitochondria and abnormal mitochondria were counted based on the collected transmission electron microscopy photos. For each treatment, at least three cells were investigated to obtain the average and standard deviation of each condition. The percentage of irregular mitochondria was therefore a good indication of a pulsing effect under the different conditions.

At the 60 and 300 ns, 60 kV/cm pulse condition, B16-F10 cells exhibited more than 40% mitochondrial irregularity with 3 or more pulses when compared with controls (Figure 9). For the 60 ns pulse duration group, fewer pulses (1 and 2 pulses) did not induce large mitochondria irregularity. With the application of more pulses, mitochondria irregularity increased to about 40% with the 3-pulse condition and approximately 60% following 4-5 pulses, with no significant difference between 4 and 5

pulse treatments. Irregularity increased and became more apparent with a longer pulse duration (300 ns), where approximately 90% of mitochondrial irregularity was found for 3-5 pulse treatments. This indicated that longer nanosecond pulse durations had a much stronger effect on B16-F10 cells. In the increased exposure time (100 μs) of the lower electric field pulse (1.2 kV/cm), B16-F10 cell mitochondria exhibited no irregularities at any of the 6 pulse treatments.

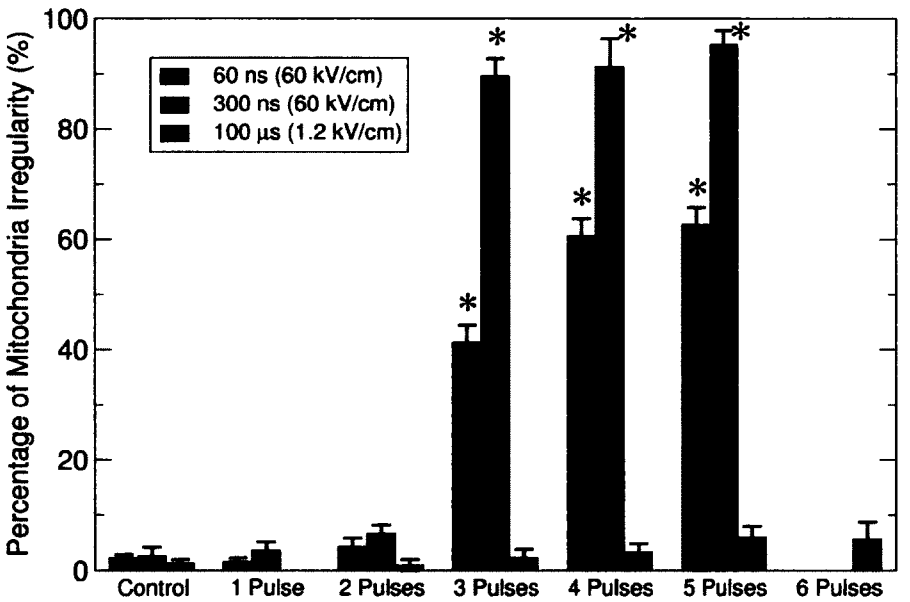

Figure 9. Percentage of mitochondrial irregularity after nanosecond (ns) and microsecond (μs) pulses
The pulse conditions of 60 kV/cm with 60 and 300 ns durations are shown in red and blue bars, respectively. Treatment under 1.2 kV/cm, 100 μs duration is shown in green. Error bars represent the standard deviation from multiple experiments. Significance compared with control group ($P \leq 0.05$) by one factor ANOVA and followed by Dunnett test is labeled with asterisk (*) on top of the bar.

3.2.2 Mitochondrial Membrane Potential Changes

Mitochondrial membrane potential ($\Delta\psi m$) is an important parameter of mitochondrial function and can be used as an indicator of cell health. In this study, $\Delta\psi m$ was tested using the fluorescent indicator JC-1, a lipophilic, cationic dye that can selectively enter into mitochondria and reversibly change color from green (monomers) to red (aggregates) as the membrane potential increases. Treated cells were incubated with JC-1 for 20 min and cells were washed and analyzed by flow cytometry 30 min post pulse. Plots represented here were taken from one of the 3 to 4 consistent replicate experiments. In the later quantitative analysis, each value was an average from three independent experiments. The contour plot showed JC-1 aggregates on the Y-axis and JC-1 monomers on the X-axis (Figure 10). In healthy cells with a high mitochondrial $\Delta\psi m$, JC-1 spontaneously formed complexes known as J-aggregates with intense red fluorescence. On the contrary, in apoptotic or unhealthy cells with low $\Delta\psi m$, JC-1 remains in the monomeric form, which showed only green fluorescence.

Figure 10 shows a typical flow cytometry diagram with the 60ns, 60 kV/cm pulse condition. For the cells without pulse treatment, the majority of the population (98.5%) fell in the Q2 area of the plot (Figure 10A), indicating the coexistence of both JC-1 aggregate and monomeric forms. As compared with the control group, cells exposed to 2 pulses exhibited the same distribution with 97.0% of the population in the Q2 area. A similar pattern was found for the 3-pulse condition (data not shown). However, with 4 and 5 pulses, JC-1 aggregates began to show a population down shift to the Q3 region, suggesting a mitochondrial potential drop in these two conditions. With these conditions, signals of the JC-1 monomeric form remained stable, since no shift along the X-axis was found.

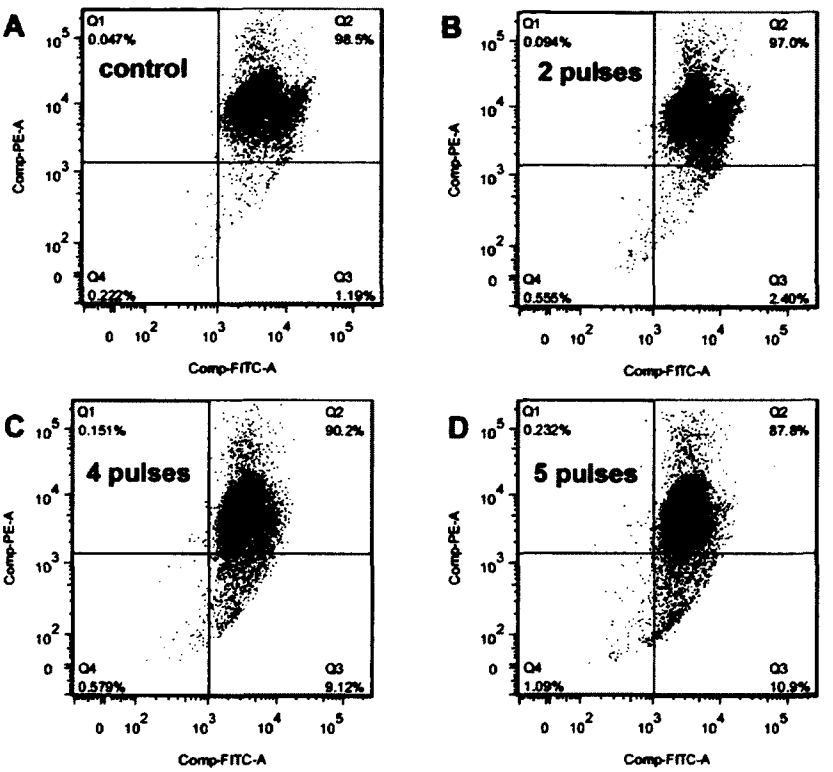

Figure 10. JC-1 analysis of B16-F10 control group and treated cells exposed to 2-5 pulses at 60 kV/cm with 60 ns duration
(A) Control group without pulsing.
(B-D) Pulse treated groups with 2, 4, and 5 pulses respectively.
JC-1 monomers are represented on the X-axis and JC-1 aggregates on the Y-axis.
Percentages of cell population of each quadrant (Q1-Q4) are shown on the corners.

For the B16-F10 cells exposed to 2-5 pulses at 60 kV/cm with 300 ns durations, no obvious effect was observed under 2 and 3 pulse conditions compared with the control group, while a decrease of JC-1 aggregate was observed with 4 and 5 pulses (Figure 11), a similar trend to the 60 ns pulse duration where the 4 and 5 pulse trials gave a population shift. Noticeably, the longer pulse duration (300 ns) had more impact on the membrane potential drop than the 60 ns pulse as represented by the larger JC-1 aggregate shift.

Especially at the 5-pulse condition, 300 ns duration had the majority (73.8%) of the cells in their JC-1 monomeric form, indicating a dramatic mitochondria potential drop, a seven fold difference as compared to the 60 ns duration with the same pulse number (10.9%). Even with 4 pulses, the shift to JC-1 monomeric form with the 300 ns pulse duration (27.3%) was three times larger than the 60 ns pulse (9.12%).

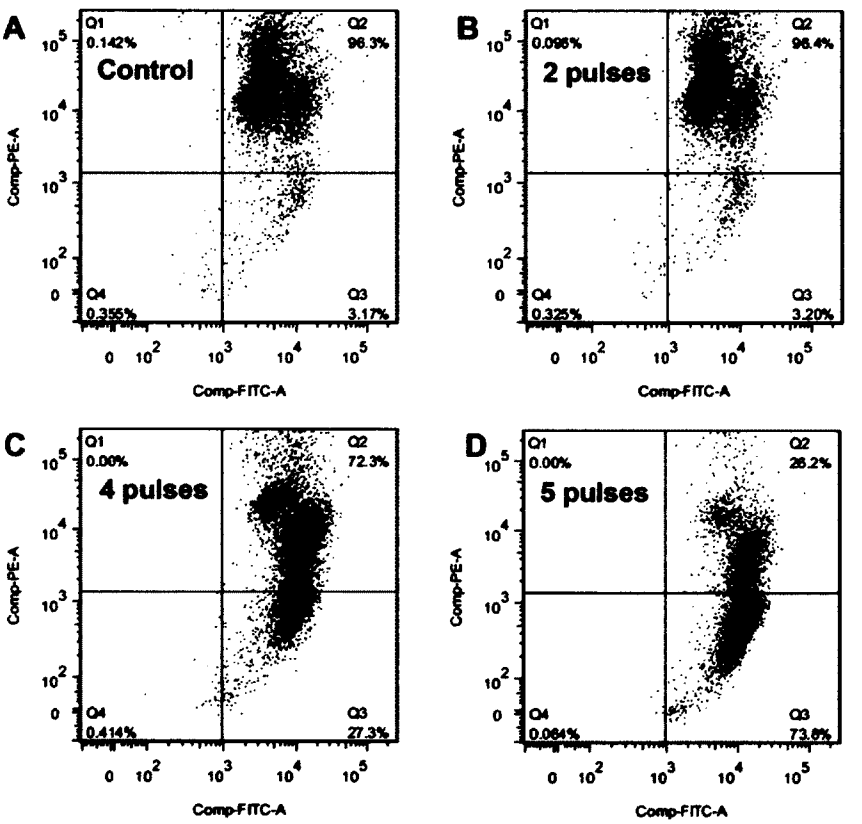

Figure 11. JC-1 analysis of B16-F10 control group and treated cells exposed to 2-5 pulses at 60 kV/cm with 300 ns duration
(A) Control group without pulsing.
(B-D) Pulse treated groups with 2-5 pulses respectively.
The contour plot shows JC-1 aggregates on the Y-axis and JC-1 monomers on the X-axis.

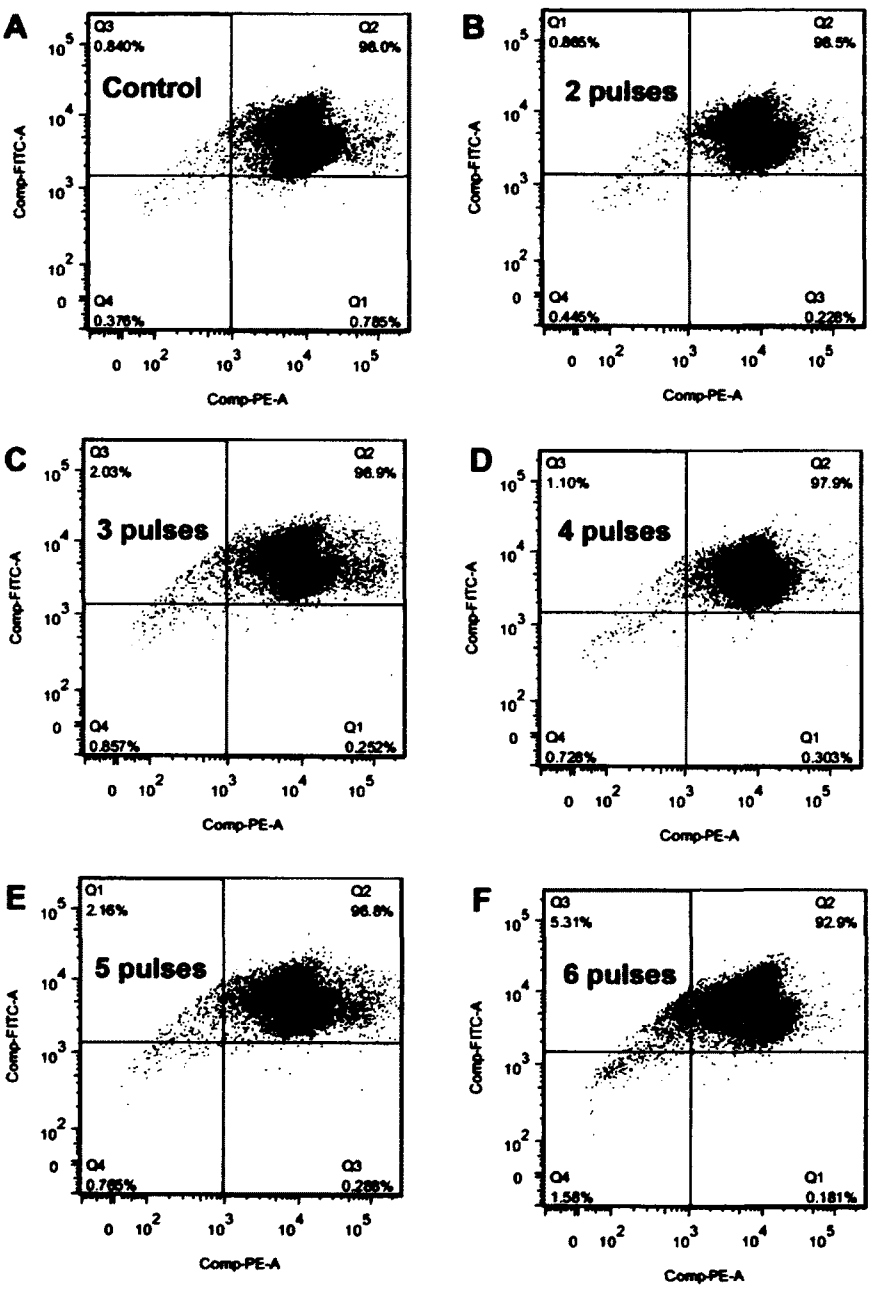

Figure 12. JC-1 analysis of B16-F10 control group and treated cells exposed to 2-6 pulses at 1.2 kV/cm with 100 μs duration
(A) Control group without pulsing.
(B-F) Pulse treated groups with 2-6 pulses respectively.
The contour plot shows JC-1 aggregates on the Y-axis and JC-1 monomers on the X-axis.

With the 100 μs 1.2kV/cm electric field, the TEM photos occasionally showed changes in the cell membrane after subjection to 6 pulses, while no mitochondria changes were suggested through 2 to 6 pulses. Therefore, we suspected there would be little or no change in the mitochondrial membrane potential at this pulsing level. As expected, patterns of JC-1 aggregates remained the same with 2-5 pulses of microsecond duration (Figure 12). With 6 pulses, there was a slight but non-significant shift of populations out of the Q2 region and into the Q3-4 region.

With a more quantitative view of the percentage of JC-1 aggregate change (Figure 13), a clear contrast could be seen among the 60 ns, 300 ns, and 100 μs pulse conditions. With microsecond pulses, JC-1 aggregate analysis indicated no observable difference between experimental and control groups. The percentage of JC-1 aggregate only dropped slightly from the control (98.05%) to 6 pulses (92.9%). While 300 ns pulse-treated groups exhibited the most significant drop of JC-1 aggregate at 4 (72.3%) and 5 (26.2%) pulsing conditions. With shorter duration, the membrane potential of 60 ns pulse treated cells began to drop slightly but with statistical significance, from 4 pulses (90.2%) to 5 pulses (87.8%).

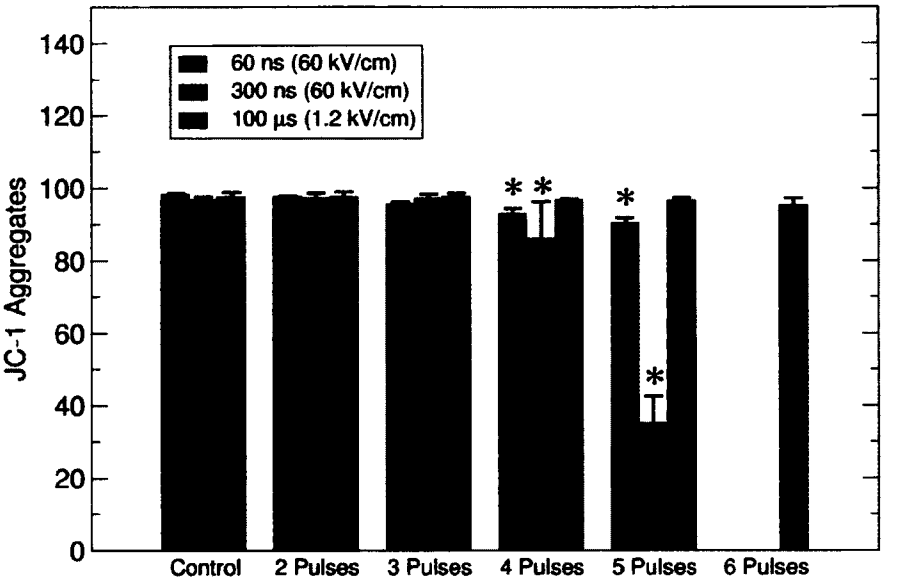

Figure 13. Quantitative analysis of JC-1 aggregates
Durations of 60 ns, 300 ns, and 100µs are displayed in red, blue, and green respectively. Error bars represent the standard deviation from multiple experiments. Significance compared with control group ($P \leq 0.05$) by one factor ANOVA and followed by Dunnett test is labeled with asterisk (*) on top of the bar.

3.3 Long-Term Cell Viability Assay

Twenty-four hours after pulse exposure, a cell survival assay was performed by using the cell hemocytometer. The cell survival data under each condition (control and pulse treated group) was an average of three replicated experiments. A percentage of over 100% reflects cell growth and division as compared to the total number of cells immediately after pulse (Figure 14). Results showed that microsecond pulses did not have a significant effect on cell viability. Note that 100 µs treated B16-F10 cells have almost identical survival profiles as the control group. Moreover, with 100 µs and 6 pulses, the cells were likely to undergo a high degree of electroporation while still maintaining full viability. With nanosecond pulse treatments, survival was affected by

the higher electric field (60 kV/cm). Cell viability at both durations (60 and 300 ns) decreased with an increase in pulse number. The significant drop in cell viability compared with the control group started with 2 pulses at both ns durations and the longer pulse duration (300 ns) had a stronger effect than the shorter duration (60 ns).

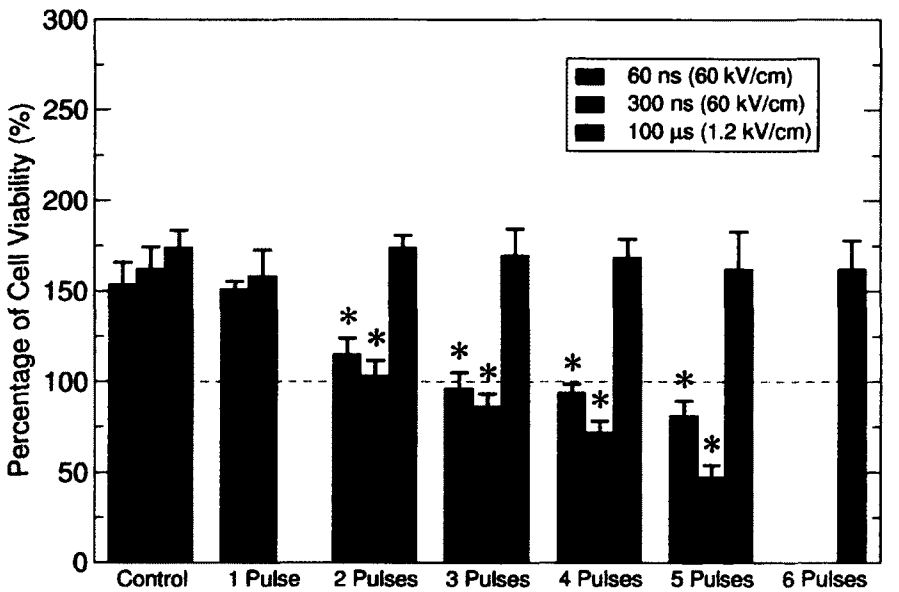

Figure 14. Percentage of cell viability 24 hrs after pulse treatment
Pulse durations of 60 ns, 300 ns, and 100 µs are displayed in red, blue, and green bar respectively. Error bars represent the standard deviation from multiple experiments. Significance compared with control group ($P \leq 0.05$) by one factor ANOVA and followed by Dunnett test is labeled with asterisk (*) on top of the bar.

3.4 Energy Density Analysis

The energy density (W) for each pulse condition could be calculated using Eq. 2 as mentioned earlier. With the increase of pulse number, energy density had a linear increase from 0 (control) to about 1×10^{-3} $\sigma_M J/cm^3\tau$ (5and 6 pulses) for the 60ns and 100 µs conditions, while the 300 ns pulse condition had a higher energy density range of 1-

5.4×10^{-3} $\sigma_M J/cm^3\tau$. When the trypan blue uptake was plotted against the energy density exerted on the cell, it was clear that higher energy density led to increased trypan blue uptake (Figure 15A). The behavior of 100 μs (0-6 pulses) and 300 ns pulse duration (0-1pulse) were similar due to the similar energy density. For the same energy density change (from 0 to 1×10^{-3} $\sigma_M J/cm^3\tau$), cells treated with 60ns pulse duration exhibited higher trypan blue uptake. This suggested larger effects on the integrity of cell outer membrane with 60 ns pulse duration under the same low energy density.

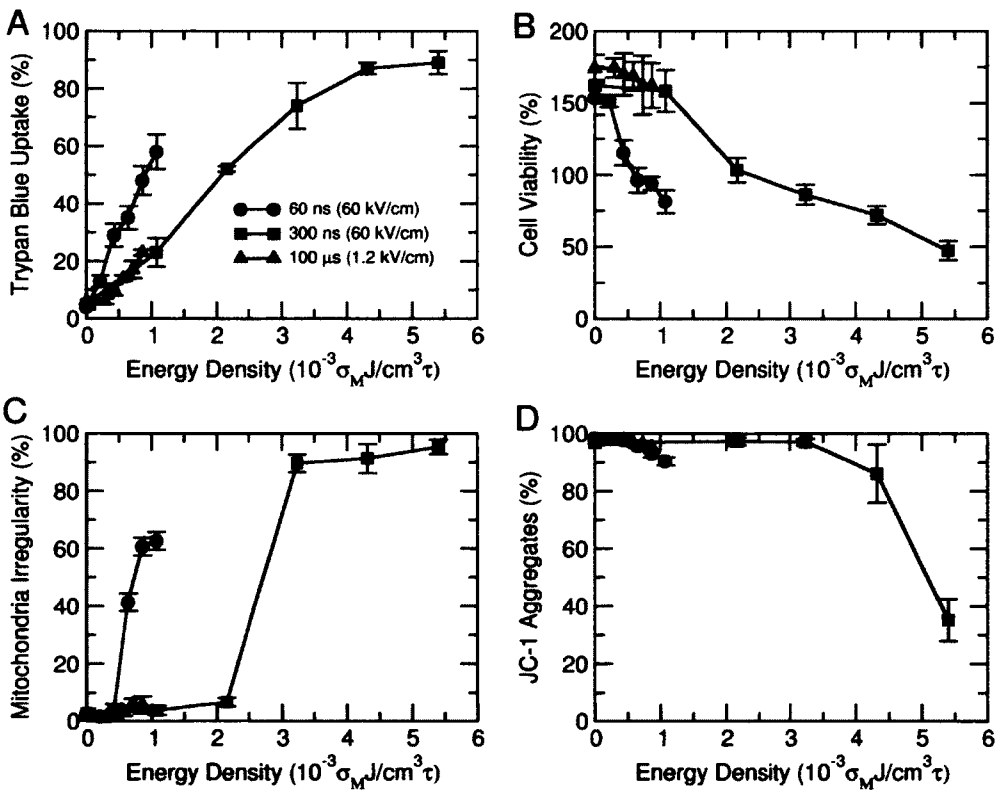

Figure 15. The relationships between cell/mitochondria properties and energy density (A-D) corresponds to the trypan blue uptake, cell viability, mitochondria irregularity, and JC-1 aggregates respectively. Pulse durations of 60 ns, 300 ns, and 100 μs are displayed in red circles, blue squares, and green triangles respectively. Error bars represent the standard deviation from multiple experiments.

Similar trends were found in the cell viability and mitochondria irregularity changes against energy density (Figure 15B, C) where 300 ns and 100 μs pulse condition exhibited overlapped curve within energy density of $0\text{-}1\times10^{-3}$ $\sigma_M J/cm^3\tau$, while 60 ns pulse condition showed increased changes. With 5 pulses of 60 ns duration, the energy density equal to 1 pulse of the 300 ns duration. However, the much higher trypan blue uptake for the 60 ns treated group (Figure 15A) as well as larger cell viability drop (Figure 15B) and mitochondria irregularity increase (Figure 15C) suggested that within the similar energy density range, cell are more vulnerable with more frequent pulses under nanosecond pulse condition, while more frequent pulses (0-6 pulses) with microsecond duration do not have much effect on the cell.

In the analysis of mitochondria membrane potential (JC-1 aggregates) against energy density (Figure 15D), the 60 ns pulse treated cells also exhibited stronger effects than the 300 ns and 100 μs pulse conditions under similar low energy density (below 1×10^{-3} $\sigma_M J/cm^3\tau$), although in a less obvious manner. This further demonstrated the greater effects with the shortest pulse (60 ns) under the same low energy density profile. A much stronger impact on mitochondria membrane potential requires more elevated energy density (above 3×10^{-3} $\sigma_M J/cm^3\tau$), suggesting a protecting mechanism within the cell or that the mitochondria structure itself was able to maintain the proper mitochondria function under stress.

CHAPTER 4

DISCUSSION

Based on the TEM analysis, no significant cell membrane morphological changes were found with nanosecond and microsecond pulse(s). The only exception was found for 100 μs, 1.2 kV/cm pulse condition where filopodial projections on cell membrane occurred at 6 pulses, suggesting comparable membrane changes as traditional electroporation under microsecond pulses. In contrast, observations on mitochondria revealed a different trend. Under nanosecond pulses (60 and 300 ns), mitochondrial irregularity started from 3 pulses with both pulse durations. While under microsecond pulses (100 μs), mitochondria shape remained normal through 2 to 6 pulses. These morphological observations clearly indicated an increased effect on intracellular organelles (mitochondria) under nanosecond pulse conditions.

These findings were in accordance with earlier studies that nsPEFs could cause breaching of intracellular granules in human blood eosinophils, while the plasma membranes remained intact (Schoenbach et al., 2001). These directly observable morphological changes and hidden variations (i.e. chemical changes which were not directly observable but measureable by chemical agents) were in close relationship with the functions of subcellular organelles. In association with mitochondrial morphological changes under the nanosecond pulse conditions, the revealed membrane potential drop by JC-1 suggested mitochondrial functional damage. In contrast, neither mitochondrial irregularity nor membrane potential drop could be found under microsecond pulses.

The examination of cell membrane changes using trypan blue uptake analysis clearly showed that 300 ns pulse duration had a much stronger effect than the 60 ns duration pulses, while the 100 μs pulses had much reduced effect and the maximum trypan blue uptake was only 23% with 6 pulses. In contrast with other studies that reported no trypan blue uptake under 600 ns, 2.4 or 4.8 kV/cm pulse condition (Pakhomov et al., 2009), our findings showed varied levels of trypan blue uptake. This difference was probably because of the different strengths of electric fields used in the two studies. Compared with the lower electric field (2.4 or 4.8 kV/cm) where no trypan blue uptake was found (Pakhomov et al., 2009), the electric field in this study (60 kV/cm) was 25 or 12.5 times greater although accompanied with shorter pulse durations (60ns and 300 ns). This suggested that both the strength of the electric field and pulse duration could affect the integrity of the cell outer membrane. However, such results required new considerations and careful interpretations as our TEM findings have demonstrated no cell membrane responses to nsPEFs.

From the cell viability analysis, it can be seen that microsecond pulses did not have any effect on cell viability and all pulse treated groups were comparable to the control group. However, increased trypan blue uptake (from 14% to 23%) was found for microsecond pulses treated cells with 4 to 6 pulses. This indicated increased cell membrane changes (electroporation) with additional pulses. The formed pores could reseal as cells treated with different number of pulses were equally viable and excluding trypan blue after 24 hrs. However, for nanosecond pulses, the increased trypan blue uptake immediately after pulse was related with decreased cell viability. Therefore, it

was not possible to directly differentiate whether trypan blue uptake resulted from pore opening or cell death.

Due to the fact that pores were not directly observed from TEM images while trypan blue uptake and cell viability data suggested such an effect under microsecond pulses, some of the following principles may apply: 1) The pore reseal time is on the scale of a few minutes, which is probably on the order of the total cell fixation time during TEM sample preparation. 2) Besides the self-reseal, the formed pores may disappear during the TEM procedure, e.g. effect of fixation. 3) The pore size may be below the current TEM resolution. The proposed nanopores, if they exist, could certainly play a significant role in nsPEF effects to destroy cancer cells as reported in earlier papers (Nuccitelli et al., 2009; Nuccitelli et al., 2006). The fact that trypan blue passed through plasma membrane under nsPEFs with increased number of pulses (Pakhomov et al., 2009; Pakhomov et al., 2007a) suggested a mix event of cell death and pore forming, and the opened pores were large enough for trypan blue uptake even though they may be beyond the resolution of our TEM scope.

Although it was not possible to differentiate trypan blue uptake from pore forming and cell death (with subsequent membrane breakdown), the data from trypan blue uptake and cell viability still suggested the existence of nanopores. With increased number of pulses (e.g. 5 pulses), fractions of cell death was around 1/2 and 2/3 for the 60 and 300 ns pulse duration respectively. However, trypan blue uptake immediately after pulse showed around 60% and 90% stained cells under these two conditions. The increased trypan blue uptake may therefore come from opened nanopores. This was also consistent with other studies where nanopores were suggested by phosphatidylserine (PS)

externalization immediately after pulse (Thomas Vernier et al., 2004). Trypan blue has a molecular weight (MW) of 872.88 Daltons and a size about 2 nm in diameter, which makes it small enough to pass through 2-3 nm diameter pores. These nanopores, being so small, would allow maintenance of membrane integrity while still allowing trypan blue to enter the living cell, which would normally not allow the trypan blue to pass. Although the outer membrane can display electroporation (larger pore size) and filopodia (6 pulses) under the 1.2 kV/cm 100 μs pulse duration, cells under this condition remained fully viable. Therefore, in contrast to internal damages that lead to increased cell death under ns pulse conditions, perturbations to the outer membrane of the cell were better tolerated.

Compared with microsecond pulses, the high electric field (60 kV/cm) and short pulse durations (60 and 300 ns) had an effect that produces demonstrable damage to the mitochondria because these ultra-short pulses were shorter than the charging time of the outer membrane and therefore had a minimal effect on the outer membrane. On the contrary, the longer duration but lower kV electric pulses were not able to trigger any mitochondrial irregularity. With a high electric field (60 kV/cm), such irregularity was induced by multiple pulses (3 and above) while not observed for fewer pulses (1 and 2). The great difference for mitochondrial irregularity between 2 pulses and 3 pulses suggested a threshold to trigger mitochondrial conformational changes. With additional pulses, cell outer membrane remained normal, and major disruption was seen in the mitochondria. When the mitochondria displayed any morphological changes (i.e. irregularity) or chemical changes (membrane potential drop), the cell viability was concurrently impaired in a rather short time period as observed in this study.

Considering the effect of nanosecond pulses on mitochondria and other cell organelles, subtle damages might occur before they could be quantitatively captured by experimental methods. As we saw under nanosecond pulses, cell viability decreased from 2 pulses and above; observable mitochondrial irregularity started from 3 pulses and above; and membrane potential drop became noticeable at 4 pulses and above. This gradation in mitochondrial responses suggested that damage to other intracellular organelles may occur prior to, or in conjunction with, mitochondrial changes that can lead to cell death from a coordinated chorus of events that overwhelm the cell. Major mitochondrial irregularity began at 3 pulses, and was in sharp contrast to results from the 2-pulse treatment. This non-linear increment suggested a threshold for triggering mitochondrial damage and also suggested a saturation point for both ns durations. Moreover, this damage was followed by a chemical change demonstrated by the membrane potential drop following 4 or more pulse treatments.

This one pulse delay between significant mitochondrial irregularity and the membrane potential drop suggested that mitochondria structures (outer membrane and/or cristae) were anatomically compromised while the membrane potential can still be maintained at the 3-pulse level. As a result, although significant mitochondria irregularity was found with 3 pulses under both nanosecond durations, the overall mitochondrial functional integrity was evidently maintained so that ion concentrations inside and outside the mitochondria still maintained at normal physiological level without drop in the membrane potential. With one additional pulse (4-pulse condition), the membrane potential was affected, i.e. the already compromised mitochondria structures were no longer able to withhold their chemical integrity. Thus, the one-pulse difference

in anatomical and physiological responses can be critical for the mitochondrial machinery needed for ATP production. When cells were under stress, mitochondrial structures were partially destroyed although they maintained the basic molecular property (membrane potential), which was essential for other functions such as producing ATP. If mitochondria membrane potential droped quickly (i.e. lost function) following structural changes, more dramatic cell death would occur than the one pulse delay mechanism which could favor cell survival under certain pulse conditions.

With fewer pulses (1-3 pulses), no significant impairment on mitochondrial potential ($\Delta\psi m$) was observed for both ns pulse durations (60 and 300ns). We would thus predict no major functional change, since this $\Delta\psi m$ was not significantly different when compared to the corresponding control groups. Meanwhile, mitochondrial structure remained unchanged with 1-2 pulses under these conditions, suggesting a close relationship between mitochondrial structure and function.

Since an electrical model predicted that as the pulse duration decreases, effects on intracellular membranes (and functions) would increase relative to effects on the outer membrane, we evaluated the effects of mitochondria membrane potential as an important secondary indicator for modulating cell function. Our experiments applying a series of pulses using B16-F10 cells that loaded with JC-1 agreed with results reported elsewhere (Beebe et al., 2003; Deng et al., 2003; Schoenbach et al., 2001) and demonstrated that nsPEFs could modulate intracellular structures and functions largely independent of effects that involve loss of plasma membrane integrity. Based on the parameters measured, such as mitochondrial irregularity, mitochondrial potential, and cell viability, nanosecond pulses had a direct impact on mitochondria. Under both pulse durations (60

and 300 ns), the mitochondria began to show irregularity from 3 pulses upward, and the membrane potential began to drop following 4 pulses. Because of these strong effects and possible damages to other organelles as mentioned earlier, cell viability was impaired from 2 pulses and steadily declined with each added pulse treatment. Also, the longer duration (300 ns) had stronger effects on mitochondrial irregularity, mitochondrial membrane potential, and cell viability than the effects seen with the shorter duration (60 ns). As suggested, the mitochondrial membrane potentials were not perturbed under the microsecond electrical fields, further demonstrating that a 100 μs pulse has more effect on the cell's plasma membrane rather than the intracellular organelles.

Results here clearly demonstrate that as the pulse duration decreases from microsecond to nanosecond, effects on the plasma membrane were minimal with only suggested nanopores while effects on intracellular organelles became dominant. This might involve calcium mobilization and apoptosis (Schoenbach et al., 2001). Thus it was possible to define nsPEF conditions that were below the threshold of plasma membrane integrity loss while control cell responses that were above or below the threshold for apoptosis at the same time. In other words, for pulse conditions below the threshold for outer membrane effects, pulse number and pulse duration could be carefully selected to determine cell function and/or fate.

Overall, the different parameters examined in this study had different relationships with regards to cell viability. Although nanosecond pulses had stronger effects on the intracellular organelles and cell viability, the steadily decreasing cell viability pattern did not correspond to the non-linear jump in mitochondrial irregularity and drop in membrane potential. However, the gradually declined cell viability with

increased pulse number was in a reverse trend with the steady increase in trypan blue uptake under the nanosecond pulse condition. This suggested that nanosecond pulse-induced cell death might be a mix effect of damages on both the plasma membrane as well as multiple intracellular organelles as mentioned earlier. Although other studies showed resistance to some of these nsPEF effects (Beebe et al., 2003), current results indicated more cells remain viable under a microsecond pulsed condition. This might originate from the different cell types used in the various studies, such as GH3, CHO-K1, and Jurkat cells which have different cell hardiness and cell membrane conductivity (a property of the latter that is related with cell membrane permeability).

In this research, we found that the effects of nsPEFs appear to be largely independent of effects on the outer cell membrane, suggesting the potential to modulate cell function by circumventing the plasma membrane and affecting cell structures and functions directly from inside the cell (i.e. regulations on intracellular organelles). We demonstrated support for the hypothesis that the cell's plasma membrane maintains its integrity while an intracellular organelle (mitochondria) could be greatly affected with nsPEFs. In addition, the effects of nsPEFs on the plasma membrane were distinct from plasma membrane electroporation although nanopores were suggested under nanosecond pulse conditions. Finally, we had presented evidence that cellular structure/function can be modulated by selectively applying PEFs that affect plasma membranes or intracellular organelles differentially.

CHAPTER 5

CONCLUSIONS

In this study we had demonstrated morphological changes on mitochondria under nanosecond electrical pulsing conditions. The evidence had been gathered both directly from TEM micrographs and electrical properties of mitochondria membranes. In summary, the low electric field (1.2 kV/cm)/long duration (100 μs) pulses might have effect on the plasma membrane at the highest pulse number with no observable or measurable damage to the mitochondria. The cell viability (μs condition) with increased pulse applications was not statistically different from the control group, which might have indicated the reseal of cell membrane electroporation after 24hrs. With high electric field (60 kV/cm), the plasma membrane maintained its integrity, while mitochondria were damaged, leading to increased cell death. As expected, the longer pulse duration (300 ns) applied more total energy and had a stronger impact than the shorter duration (60 ns) on all the monitored parameters.

The mitochondrial membrane potential drop followed the observed appearance of mitochondrial irregularity. This phenomenon was observed only when mitochondrial irregularity became significant and had a 1-pulse delay from the irregularity response. In contrast, with microsecond pulses (100 μs) the effect was shielded by the outer membrane, and therefore no irregularity changes or mitochondrial membrane potential drops were observed for the microsecond pulses. Although no pore opening was observed under the experimental conditions in this study, the trypan blue uptake and cell

viability test suggested an electroporation and pore reseal event with μs pulses and a mix event of both cell death and pore forming with ns pulses. With the elevated trypan blue uptake under the ns pulses, this type of "hidden" poration might also play a role in the cell viability which involves intracellular organelle damages.

When comparing the energy density exerted on the cell under different pulse conditions, the 60 kV/cm electric field with 300 ns pulse duration had the most intense energy density which reached up to 5.4×10^{-3} $\sigma_M J/cm^3\tau$ with 5 pulses and larger physical/chemical changes were associated with the energy density above 3×10^{-3} $\sigma_M J/cm^3\tau$. Under similar low energy density (below 1×10^{-3} $\sigma_M J/cm^3\tau$), effects of 300 ns and 100 μs pulse durations were similar, although cells were subjected to different pulse number (1 pulse for 300 ns and 6 pulses for 100 μs). However, 60 ns pulse treated cells under the same low energy density profile exhibited a much stronger effect. Clearly, with respect to the same energy density, the shortest pulse duration (60 ns) in this study had the most significant impact on cell membrane permeability and cell survivability. And such effects were likely to result from changes/damages on subcellular structures such as mitochondria.

REFERENCES

Abiror, I.G., Arakelyan, V.B., Chernomordik, L.V., Chizmadzhev, Y.A., Pastushenko, V.F., and Tarasevich, M.R. (1979). Electric breakdown of bilayer lipid membranes I. the main experimental facts and their qualitative discussion. Bioelectrochem. Bioenerget. *6*, 37-52.

Alberts, B., Johnson, A., Lewis, J., Raff, M., Roberts, K., and Walter, P. (2002). Molecular Biology of the Cell 4th ed (New York: Garland Science).

Bartoletti, D.C., Harrison, G.I., and Weaver, J.C. (1989). The number of molecules taken up by electroporated cells: quantitative determination. FEBS Lett. *256*, 4-10.

Beebe, S.J., Fox, P.M., Rec, L.J., Somers, K., Stark, R.H., and Schoenbach, K.H. (2002). Nanosecond pulsed electric field (nsPEF) effects on cells and tissues: apoptosis induction and tumor growth inhibition. IEEE T. Plasma Sci. *30*, 286-292.

Beebe, S.J., White, J., Blackmore, P.F., Deng, Y., Somers, K., and Schoenbach, K.H. (2003). Diverse effects of nanosecond pulsed electric fields on cells and tissues. DNA Cell Biol. *22*, 785-796.

Benz, R., Beckers, F., and Zimmermann, U. (1979). Reversible electrical breakdown of lipid bilayer membranes: a charge-pulse relaxation study. J. Membr. Biol. *48*, 181-204.

Berglund, D.L., and Starkey, J.R. (1989). Isolation of viable tumor cells following introduction of labelled antibody to an intracellular oncogene product using electroporation. J. Immunol. Methods *125*, 79-87.

Buescher, E.S., and Schoenbach, K.H. (2003). Effects of submicrosecond, high intensity pulsed electric fields on living cells - intracellular electromanipulation. IEEE T. Dielect. El. In. *10*, 788-794.

Chen, N., Garner, A.L., Chen, G., Jing, Y., Deng, Y., Swanson, R.J., Kolb, J.F., Beebe, S.J., Joshi, R.P., and Schoenbach, K.H. (2007). Nanosecond electric pulses penetrate the nucleus and enhance speckle formation. Biochem. Biophys. Res. Commun. *364*, 220-225.

Chipuk, J.E., Bouchier-Hayes, L., and Green, D.R. (2006). Mitochondrial outer membrane permeabilization during apoptosis: the innocent bystander scenario. Cell Death Differ. *13*, 1396-1402.

Cole, K.S. (1937). Electric impedance of marine egg membranes. T. Faraday Soc. *33*, 966-972.

Crowley, J.M. (1973). Electrical breakdown of bimolecular lipid membranes as an electromechanical instability. Biophys. J. *13*, 711-724.

Davalos, R., Mir, L., and Rubinsky, B. (2005). Tissue ablation with irreversible electroporation. Ann. Biomed. Eng. *33*, 223-231.

Deng, J., Schoenbach, K.H., Stephen Buescher, E., Hair, P.S., Fox, P.M., and Beebe, S.J. (2003). The effects of intense submicrosecond electrical pulses on cells. Biophys. J. *84*, 2709-2714.

Di Lisa, F., Blank, P.S., Colonna, R., Gambassi, G., Silverman, H.S., Stern, M.D., and Hansford, R.G. (1995). Mitochondrial membrane potential in single living adult rat cardiac myocytes exposed to anoxia or metabolic inhibition. J. Physisol. *486*, 1-13.

Diederich, A., Bahr, G., and Winterhalter, M. (1998). Influence of surface charges on the rupture of black lipid membranes. Phys. Rev. E *58*, 4883 - 4889.

Dimitrov, D.S. (1984). Electric field-induced breakdown of lipid bilayers and cell membranes: a thin viscoelastic film model. J. Membr. Biol. *78*, 53-60.

Erni, R., Rossell, M.D., Kisielowski, C., and Dahmen, U. (2009). Atomic-resolution imaging with a sub-50-pm electron probe. Phys. Rev. Lett. *102*, 096101.

Gardner, A., and Boles, R.G. (2005). Is a "mitochondrial psychiatry" in the future? a review. Curr. Psychiatry Rev. *1*, 255-271.

Gift, E.A., and Weaver, J.C. (2000). Simultaneous quantitative determination of electroporative molecular uptake and subsequent cell survival using gel microdrops and flow cytometry. Cytometry *39*, 243-249.

Glaser, R.W., Leikin, S.L., Chernomordik, L.V., Pastushenko, V.F., and Sokirko, A.I. (1988). Reversible electrical breakdown of lipid bilayers: formation and evolution of pores. BBA-Biomembranes *940*, 275-287.

Golzio, M., Teissié, J., and Rols, M.-P. (2002). Direct visualization at the single-cell level of electrically mediated gene delivery. Proc. Natl. Acad. Sci. USA *99*, 1292-1297.

Graziadei, L., Burfeind, P., and Bar-Sagi, D. (1991). Introduction of unlabeled proteins into living cells by electroporation and isolation of viable protein-loaded cells using dextran-fluorescein isothiocyanate as a marker for protein uptake. Anal. Biochem. *194*, 198-203.

Hair, P.S., Schoenbach, K.H., and Buescher, E.S. (2003). Sub-microsecond, intense pulsed electric field applications to cells show specificity of effects. Bioelectrochemistry *61*, 65-72.

Harrison, R.L., Byrne, B.J., and Tung, L. (1998). Electroporation-mediated gene transfer in cardiac tissue. FEBS Lett. *435*, 1-5.

Hayashi, T., Rizzuto, R., Hajnoczky, G., and Su, T.-P. (2009). MAM: more than just a housekeeper. Trends Cell Biol. *19*, 81-88.

Heller, L.C., and Heller, R. (2006). In vivo electroporation for gene therapy. Hum. Gene Ther. *17*, 890-897.

Heller, R., Jaroszeski, M., Atkin, A., Moradpour, D., Gilbert, R., Wands, J., and Nicolau, C. (1996). In vivo gene electroinjection and expression in rat liver. FEBS Lett. *389*, 225-228.

Henze, K., and Martin, W. (2003). Evolutionary biology: essence of mitochondria. Nature *426*, 127-128.

Herrmann, J.M., and Neupert, W. (2000). Protein transport into mitochondria. Curr. Opin. Microbiol. *3*, 210-214.

Hibino, M., Shigemori, M., Itoh, H., Nagayama, K., and Kinosita, K. (1991). Membrane conductance of an electroporated cell analyzed by submicrosecond imaging of transmembrane potential. Biophys. J. *59*, 209-220.

Hu, Q., Viswanadham, S., Joshi, R.P., Schoenbach, K.H., Beebe, S.J., and Blackmore, P.F. (2005). Simulations of transient membrane behavior in cells subjected to a high-intensity ultrashort electric pulse. Phys. Rev. E *71*, 031914.

Jansen, M., and Blume, A. (1995). A comparative study of diffusive and osmotic water permeation across bilayers composed of phospholipids with different head groups and fatty acyl chains. Biophys. J. *68*, 997-1008.

Joshi, R.P., Hu, Q., Aly, R., Schoenbach, K.H., and Hjalmarson, H.P. (2001). Self-consistent simulations of electroporation dynamics in biological cells subjected to ultrashort electrical pulses. Phys. Rev. E *64*, 011913.

Joshi, R.P., Hu, Q., Schoenbach, K.H., and Hjalmarson, H.P. (2002). Improved energy model for membrane electroporation in biological cells subjected to electrical pulses. Phys. Rev. E *65*, 041920.

Joshi, R.P., and Schoenbach, K.H. (2000). Electroporation dynamics in biological cells subjected to ultrafast electrical pulses: A numerical simulation study. Phys. Rev. E *62*, 1025.

Keese, C.R., Wegener, J., Walker, S.R., and Giaever, I. (2004). Electrical wound-healing assay for cells in vitro. Proc. Natl. Acad. Sci. USA *101*, 1554-1559.

Kolb, J.F., Kono, S., and Schoenbach, K.H. (2006). Nanosecond pulsed electric field generators for the study of subcellular effects. Bioelectromagnetics *27*, 172-187.

Kulkarni, G.V., Lee, W., Seth, A., and McCulloch, C.A.G. (1998). Role of mitochondrial membrane potential in concanavalin A-Induced apoptosis in human fibroblasts. Exp. Cell Res. *245*, 170-178.

Lee, R.C., River, L.P., Pan, F.S., Ji, L., and Wollmann, R.L. (1992). Surfactant-induced sealing of electropermeabilized skeletal muscle membranes in vivo. Proc. Natl. Acad. Sci. USA *89*, 4524-4528.

Lesnefsky, E.J., Moghaddas, S., Tandler, B., Kerner, J., and Hoppel, C.L. (2001). Mitochondrial Dysfunction in Cardiac Disease: Ischemia-Reperfusion, Aging, and Heart Failure. J. Mol. Cell. Cardiol. *33*, 1065-1089.

Lukas, J., Bartek, J., and Strauss, M. (1994). Efficient transfer of antibodies into mammalian cells by electroporation. J. Immunol. Methods *170*, 255-259.

Lundqvist, J.A., Sahlin, F., Åberg, M.A.I., Strömberg, A., Eriksson, P.S., and Orwar, O. (1998). Altering the biochemical state of individual cultured cells and organelles with ultramicroelectrodes. Proc. Natl. Acad. Sci. USA *95*, 10356-10360.

Mancini, M., Anderson, B.O., Caldwell, E., Sedghinasab, M., Paty, P.B., and Hockenbery, D.M. (1997). Mitochondrial proliferation and paradoxical membrane depolarization during terminal differentiation and apoptosis in a human colon carcinoma cell line. J. Cell Biol. *138*, 449-469.

Mariana, R.V. (2006).
http://en.wikipedia.org/wiki/File:Animal_mitochondrion_diagram_en_(edit).svg

McBride, H.M., Neuspiel, M., and Wasiak, S. (2006). Mitochondria: more than just a powerhouse. Curr. Biol. *16*, R551-R560.

Mir, L.M. (2001). Therapeutic perspectives of in vivo cell electropermeabilization. Bioelectrochemistry *53*, 1-10.

Mir, L.M., Orlowski, S., Belehradek, J., Teissi, J., Rols, M.P., Sersa, G., Miklavcic, D., Gilbert, R., and Heller, R. (1995). Biomedical applications of electric pulses with special emphasis on antitumor electrochemotherapy. Bioelectrochem. Bioenerget. *38*, 203-207.

Mir, L.M., Orlowski, S., Belehradek Jr, J., and Paoletti, C. (1991). Electrochemotherapy potentiation of antitumour effect of bleomycin by local electric pulses. Eur. J. Cancer Clin. On. *27*, 68-72.

Moore, J.W. (1969). Membranes, ions and impulses. a chapter of classical biophysics. Science *163*, 268.

Needham, D., and Hochmuth, R.M. (1989). Electro-mechanical permeabilization of lipid vesicles. role of membrane tension and compressibility. Biophys. J. *55*, 1001-1009.

Neumann, E., Kakorin, S., Tsoneva, I., Nikolova, B., and Tomov, T. (1996). Calcium-mediated DNA adsorption to yeast cells and kinetics of cell transformation by electroporation. Biophys. J. *71*, 868 - 877.

Neumann, E., Schaefer-Ridder, M., Wang, Y., and Hofschneider, P.H. (1982). Gene transfer into mouse lyoma cells by electroporation in high electric fields. EMBO J. *1*, 841-845.

Nuccitelli, R., Chen, X., Pakhomov, A.G., Baldwin, W.H., Sheikh, S., Pomicter, J.L., Ren, W., Osgood, C., Swanson, R.J., Kolb, J.F., *et al.* (2009). A new pulsed electric field therapy for melanoma disrupts the tumor's blood supply and causes complete remission without recurrence. Int. J. Cancer *125*, 438-445.

Nuccitelli, R., Pliquett, U., Chen, X., Ford, W., James Swanson, R., Beebe, S.J., Kolb, J.F., and Schoenbach, K.H. (2006). Nanosecond pulsed electric fields cause melanomas to self-destruct. Biochem. Biophys. Res. Commun. *343*, 351-360.

Pakhomov, A.G., Bowman, A.M., Ibey, B.L., Andre, F.M., Pakhomova, O.N., and Schoenbach, K.H. (2009). Lipid nanopores can form a stable, ion channel-like conduction pathway in cell membrane. Biochem. Biophys. Res. Commun. *385*, 181-186.

Pakhomov, A.G., Kolb, J.F., White, J.A., Joshi, R.P., Xiao, S., and Schoenbach, K.H. (2007a). Long-lasting plasma membrane permeabilization in mammalian cells by nanosecond pulsed electric field (nsPEF). Bioelectromagnetics *28*, 655-663.

Pakhomov, A.G., Shevin, R., White, J.A., Kolb, J.F., Pakhomova, O.N., Joshi, R.P., and Schoenbach, K.H. (2007b). Membrane permeabilization and cell damage by ultrashort electric field shocks. Arch. Biochem. Biophys. *465*, 109-118.

Potts, R.O., and Francoeur, M.L. (1990). Lipid biophysics of water loss through the skin. Proc. Natl. Acad. Sci. USA *87*, 3871-3873.

Prausnitz, M.R., Lau, B.S., Milano, C.D., Conner, S., Langer, R., and Weaver, J.C. (1993). A quantitative study of electroporation showing a plateau in net molecular transport. Biophys. J. *65*, 414-422.

Reers, M., Smith, T.W., and Chen, L.B. (1991). J-aggregate formation of a carbocyanine as a quantitative fluorescent indicator of membrane potential. Biochemistry *30*, 4480-4486.

Rols, M., Delteil, C., Golzio, M., Dumond, P., Cros, S., and Teissie, J. (1998). In vivo electrically mediated protein and gene transfer in murine melanoma. Nat. Biotechnol. *16*, 168 - 171.

Schoenbach, K.H., Beebe, S.J., and Buescher, E.S. (2001). Intracellular effect of ultrashort electrical pulses. Bioelectromagnetics *22*, 440-448.

Schoenbach, K.H., Hargrave, B., Joshi, R.P., Kolb, J.F., Nuccitelli, R., Osgood, C., Pakhomov, A., Stacey, M., Swanson, R.J., White, J.A., *et al.* (2007). Bioelectric Effects of Intense Nanosecond Pulses. Dielectrics and Electrical Insulation, IEEE Transactions on *14*, 1088-1109.

Schoenbach, K.H., Joshi, R.P., Kolb, J.F., Chen, N., Stacey, M., Buescher, E.S., Beebe, S.J., and Blackmore, P. (2004). Ultrashort electrical pulses open a new gateway into biological cells. Paper presented at: Power Modulator Symposium, 2004 and 2004 High-Voltage Workshop. Conference Record of the Twenty-Sixth International.

Schwan, H.P. (1968). Electrode polarization impedance and measurements in biological materials. Ann. N. Y. Acad. Sci. *148*, 191-209.

Sersa, G., Cemazar, M., Miklavcic, D., and Mir, L.M. (1994). Electrochemotherapy: variable anti-tumor effect on different tumor models. Bioelectrochem. Bioenerget. *35*, 23-27.

Sersa, G., Miklavcic, D., Cemazar, M., Rudolf, Z., Pucihar, G., and Snoj, M. (2008). Electrochemotherapy in treatment of tumours. Eur. J. Surg. Oncol. *34*, 232-240.

Sick, T.J., and Perez-Pinzon, M.A. (1999). Optical Methods for Probing Mitochondrial Function in Brain Slices. Methods *18*, 104-108.

Singer, S.J., and Nicolson, G.L. (1972). The fluid mosaic model of the structure of cell membranes. Science *175*, 720-731.

Smiley, S.T., Reers, M., Mottola-Hartshorn, C., Lin, M., Chen, A., Smith, T.W., Steele, G.D., and Chen, L.B. (1991). Intracellular heterogeneity in mitochondrial membrane potentials revealed by a J-aggregate-forming lipophilic cation JC-1. Proc. Natl. Acad. Sci. USA *88*, 3671-3675.

Stacey, M., Stickley, J., Fox, P., Statler, V., Schoenbach, K., Beebe, S.J., and Buescher, S. (2003). Differential effects in cells exposed to ultra-short, high intensity electric fields: cell survival, DNA damage, and cell cycle analysis. Mutat. Res.-Genet. Toxicol. Environ. Mutag. *542*, 65-75.

Strober, W. (1997). Trypan Blue Exclusion Test of Cell Viability. (New York: John Wiley & Sons).

Teissi, J., Eynard, N., Gabriel, B., and Rols, M.P. (1999). Electropermeabilization of cell membranes. Adv. Drug Del. Rev. *35*, 3-19.

Tekle, E., Oubrahim, H., Dzekunov, S.M., Kolb, J.F., Schoenbach, K.H., and Chock, P.B. (2005). Selective field effects on intracellular vacuoles and vesicle membranes with nanosecond electric pulses. Biophys. J. *89*, 274-284.

Thomas Vernier, P., Sun, Y., Marcu, L., Craft, C.M., and Gundersen, M.A. (2004). Nanoelectropulse-induced phosphatidylserine translocation. Biophys. J. *86*, 4040-4048.

Tieleman, D.P. (2004). The molecular basis of electroporation. BMC Biochem. *5*, 10.

Titomirov, A.V., Sukharev, S., and Kistanova, E. (1991). In vivo electroporation and stable transformation of skin cells of newborn mice by plasmid DNA. BBA-Gene Struct. Expr. *1088*, 131-134.

Tsong, T.Y. (1991). Electroporation of cell membranes. Biophys. J. *60*, 297-306.

Uno, I., Fukami, K., Kato, H., Takenawa, T., and Ishikawa, T. (1988). Essential role for phosphatidylinositol 4,5-bisphosphate in yeast cell proliferation. Nature *333*, 188-190.

Vernier, P.T., Sun, Y., Marcu, L., Salemi, S., Craft, C.M., and Gundersen, M.A. (2003). Calcium bursts induced by nanosecond electric pulses. Biochem. Biophys. Res. Commun. *310*, 286-295.

Verspohl, E.J., Kaiserling-Buddemeier, I., and Wienecke, A. (1997). Introducing specific antibodies into electropermeabilized cells is a valuable tool for eliminating specific cell functions. Cell Biochem. Funct. *15*, 127-134.

Wadia, J.S., Chalmers-Redman, R.M.E., Ju, W.J.H., Carlile, G.W., Phillips, J.L., Fraser, A.D., and Tatton, W.G. (1998). Mitochondrial Membrane Potential and Nuclear Changes in Apoptosis Caused by Serum and Nerve Growth Factor Withdrawal: Time Course and Modification by (-)-Deprenyl. J. Neurosci. *18*, 932-947.

Wang, S., Chen, J., Chen, M.-T., Vernier, P.T., Gundersen, M.A., and Valderrábano, M. (2009). Cardiac Myocyte Excitation by Ultrashort High-Field Pulses. Biophys. J. *96*, 1640-1648.

Weaver, J.C. (1993). Electroporation: a general phenomenon for manipulating cells and tissues. J Cell Biochem *51*, 426-435.

Weaver, J.C. (1995). Electroporation Theory: Concepts and Mechanisms. In Plant Cell Electroporation and Electrofusion Protocols (New York, Humana Press), pp. 3-28.

Weaver, J.C. (2000). Electroporation of cells and tissues. IEEE T. Plasma Sci. *28*, 24-33.

Weaver, J.C. (2003). Electroporation of biological membranes from multicellular to nano scales. IEEE T. Dielect. El. In. *10*, 754-768.

Weaver, J.C., and Chizmadzhev, Y.A. (1996). Theory of electroporation: a review. Bioelectrochem. Bioenerget. *41*, 135-160.

White, J.A., Blackmore, P.F., Schoenbach, K.H., and Beebe, S.J. (2004). Stimulation of capacitative calcium entry in HL-60 cells by nanosecond pulsed electric fields. J. Biol. Chem. *279*, 22964-22972.

White, R.J., and Reynolds, I.J. (1996). Mitochondrial depolarization in glutamate-stimulated neurons: an early signal specific to excitotoxin exposure. J. Neurosci. *16*, 5688-5697.

Zimmermann, U. (1996). The Effect of High Intensity Electric Field Pulses on Eukaryotic Cell Membranes: Fundamentals and Applications. In Electromanipulation of cells (USA, CRC Press).

Zimmermann, U., Pilwat, G., Beckers, F., and Riemann, F. (1976). Effects of external electrical fields on cell membranes. Bioelectrochem. Bioenerget. *3*, 58-83.

VITA

Yiling Chen

Education

- Old Dominion University
  Department of Biological Science
  Hampton Blvd. Norfolk, VA 23529
  Ph.D. in Biomedical Sciences, Spring 2012

- The University of Nottingham
  School of Clinical Sciences
  Queen's Medical Centre, Nottingham, NG7 2UH
  MS. in Molecular Medical Microbiology, Aug 2004

- Tianjin Medical University
  Department of Medicine
  No. 22 Qixiangtai Road, Heping District Tianjin 300070
  MD. in Medicine, Fall 2001

Presentations

• 2010 ASB Annual Meeting in Asheville	*Poster*	2010.04
• 7th International Bioelectrics Symposium in Norfolk	*Poster*	2010.06
• 50th ASCB Annual Meeting in Philadelphia.	*Poster*	2010.12